2015

Association of Autophagy in the Cell Death Mediated by Dihydrotestosterone in Autoreactive T Cells Independent of Antigenic Stimulation

Ting Jia
University of Nebraska-Lincoln, tjia2@unl.edu

Annandurai Anandhan
University of Nebraska-Lincoln, aanandhan@unl.edu

Chandirasegaran Massilamany
University of Nebraska-Lincoln, cmassilamany@unl.edu

Rajkumar A. Rajasekaran
University of Nebraska-Lincoln, rajkumar.ar@unl.edu

Rodrigo Franco
University of Nebraska-Lincoln, rfrancocruz2@unl.edu

See next page for additional authors

Published in *Journal of Neuroimmune Pharmacology* 10 (2015), pp. 620–634; doi: 10.1007/s11481-015-9633-x

Submitted April 29, 2015; accepted September 15, 2015; published online September 29, 2015.

Association of Autophagy in the Cell Death Mediated by Dihydrotestosterone in Autoreactive T Cells Independent of Antigenic Stimulation

Ting Jia, Annandurai Anandhan, Chandirasegaran Massilamany, Rajkumar A. Rajasekaran, Rodrigo Franco, and Jay Reddy

School of Veterinary Medicine and Biomedical Sciences, University of Nebraska-Lincoln

Corresponding author — Jay Reddy, Room 202, Bldg. VBS, Lincoln, NE 68583, USA; nreddy2@unl.edu

Abstract

Gender disparity is well documented in the mouse model of experimental autoimmune encephalomyelitis (EAE) induced with proteolipid protein (PLP) 139–151, in which female, but not male, SJL mice show a chronic relapsing-remitting paralysis. Furthermore, dihydrotestosterone (DHT) has been shown to ameliorate the severity of EAE, but the underlying mechanisms of its protective effects are unclear. Using major histocompatibility complex (MHC) class II dextramers for PLP 139-151, we tested the hypothesis that DHT selectively modulates the expansion and functionalities of antigen-specific T cells. Unexpectedly, we noted that DHT induced cell death in antigen-specific, autoreactive T cells, but the effects were not selective, because both proliferating and non-proliferating cells were equally affected independent of antigenic stimulation. Furthermore, DHT-exposed PLP 139- 151-specific T cells did not show any shift in cytokine production; rather, frequencies of cytokine-producing PLP-specific T cells were significantly reduced, irrespective of T helper (Th) 1, Th2, and Th17 subsets of cytokines. By evaluating cell death and autophagy pathways, we provide evidence for the induction of autophagy to be associated with cell death caused by DHT. Taken together, the data provide new insights into the role of DHT and indicate that cell death and autophagy contribute to the therapeutic effects of androgens in autoreactive T cells.

Keywords: DHT, Myelin proteolipid protein, MHC class II dextramers, Autoreactive T cells, Apoptosis, Autophagy

Introduction

Multiple sclerosis (MS) is thought to be an autoimmune disease, but the antigens that induce it are unknown (Haegert and Marrosu 1994). Although men are less likely than women to develop MS, they tend to develop a more severe, chronic form of the disease (Compston et al. 2006). Disease severity in female MS patients is reduced during pregnancy, but the symptoms of MS return to their pre-pregnant state within 6 months post-delivery (Confavreux et al. 1998). Furthermore, reduced severity of MS during pregnancy is correlated with higher estriol levels, and oral estriol treatment of relapsing-remitting MS patients reduces the number of enhancing lesions seen on magnetic resonance imaging (Soldan et al. 2003). Such an alteration in the disease course, although attributed to elevated amounts of T helper (Th) 2 cytokines during pregnancy, may be due to additional factors.

To determine the mechanisms of gender differences in susceptibility to central nervous system (CNS) autoimmunity, mouse models of experimental autoimmune encephalomyelitis (EAE) are commonly employed. EAE can be induced by immunizing susceptible mouse strains with the CNS myelin antigens, which include myelin proteolipid protein (PLP), myelin basic protein (MBP), and myelin oligodendrocyte glycoprotein (MOG), or their corresponding immunogenic peptide fragments PLP 139-151, MBP 89-101/MBP Ac1-11, and MOG 35-55 in complete Freund's adjuvant (Miller et al. 2007; Constantinescu et al. 2011; McCarthy et al. 2012). While gender bias in susceptibility to EAE

has been noted with both PLP and MBP antigens, EAE induced with PLP 139-151 has been commonly used, because it results in manifestations of the disease phenotypes that are distinct by gender: only females develop chronic relapsing-remitting paralysis (Bebo et al. 1996). However, clinical relapses could be induced in males by orchidectomy, pointing to the pivotal role androgens play in the regulation of CNS autoimmunity (Bebo et al. 1998). Consistent with this notion, the therapeutic efficacy of androgens has been tested in EAE, with the result that both dihydrotestosterone (DHT) and dihydroepiandrosterone have been shown to ameliorate the severity of EAE when administered either during the induction or effector phase of the disease (Dalal et al. 1997; Du et al. 2001; Palaszynski et al. 2004). Additionally, female mice treated with DHT experience less severe EAE accompanied by enhanced interleukin (IL)-10 production (Dalal et al. 1997). These observations suggest that androgens act on T cells and may mediate anti-inflammatory effects. In support of this hypothesis, expression of an androgen receptor has been demonstrated in splenocytes and thymocytes in mice and humans (Kovacs and Olsen 1987; Benten et al. 1999; Benten et al. 2002).

Furthermore, using the EAE adoptive transfer protocol, we and others have demonstrated that PLP 139-151-reactive T cells generated in male SJL mice induce EAE in females, but severity is low and the clinical signs of EAE take a long time to appear. On the contrary, cells from female mice induce EAE in males with a disease severity comparable to its severity in female recipients of female cells (Bebo et al. 1999; Massilamany et al. 2011b). These data suggest that male hormones play an important role in controlling autoimmune responses. Because PLP 139-151-induced EAE is classically a CD4 T cell-mediated disease, any immunomodulatory effects exerted from the use of androgens are expected to influence mainly this subset of T cells. Consistent with this notion, DHT treatment of myelin-reactive T cells has led to deviation of immune response from a proinflammatory (Th1) toward an anti-inflammatory (Th2) environment by promoting the induction of IL-10 (Dalal et al. 1997; Bebo et al. 1999; Liva and Voskuhl 2001). However, it was not known whether such a deviation occurred in antigen-specific T cells or indirectly by affecting non-antigen-specific T cells. To address this question, we recently created the next generation of major histocompatibility complex (MHC) class II tetramers called dextramers for PLP 139-151, permitting us to enumerate the frequencies of PLP-specific CD4 T cells in various experimental systems (Massilamany et al. 2011c; Gangaplara et al. 2012). In this report, we made efforts to determine the functionalities of DHT by analyzing the frequencies of PLP specific T cells, leading us to the unexpected finding that DHT acts by depleting T cells through cell death which was found to be associated with autophagy. The effects were not selective, in that both proliferating and non-proliferating cells were equally affected, independent of antigenic stimulation, but with no shift in the production of cytokines.

Materials and Methods

Mice

Five-to-six-week-old male and female SJL/J (H-2^s) mice were procured from the Jackson Laboratory (Bar Harbor, ME). The mice were maintained according to the animal protocol guidelines of the University of Nebraska–Lincoln, Lincoln, NE.

Peptide Synthesis and Immunization Procedures

PLP 139-151 (HSLGKWLGHPDKF) and neuraminidase (NASE) 101–120 (EALVRQGLAKVAYVYKPNNT) were synthesized on 9-fluorenylmethyloxycarbonyl chemistry (Neopeptide, Cambridge, MA). All peptides were HPLC-purified (>90 %), identity was confirmed by mass spectroscopy, and the peptides were dissolved in 1 × phosphate-buffered saline (PBS) prior to use. To generate primary T cell cultures for PLP 139-151, SJL mice were immunized subcutaneously (s.c.) with PLP 139-151 emulsified in complete Freund's adjuvant in multiple sites in the inguinal flank and sternal regions (100 μg/ mouse) (Miller et al. 2007; Massilamany et al. 2010).

T Cell Proliferative Assay

Single-cell suspensions were prepared from the draining lymph nodes, hereafter termed lymph node cells (LNCs), from PLP-immunized mice on day 10 post-immunization or from naïve mice, and the cell pellets were resuspended in 1 × ammonium chloride potassium buffer (Lonza, Walkersville, MD) to lyse erythrocytes as described (Massilamany et al. 2011a). After washing, cell pellets were resuspended in RPMI medium supplemented with 10 % fetal bovine serum (FBS), 1 mM sodium pyruvate, 4 mM L-glutamine, 1 × each of nonessential amino acids and vitamin mixture, and 100 U/ml penicillin-streptomycin (Lonza; hereafter called growth medium). Cell viability was verified by trypan blue staining. Cells from immunized mice were stimulated at a density of 5×10^6 cells/ml in triplicates with the indicated peptides (0 to 80 μg/ml) for 2 days in growth medium in the presence or absence of DHT (Sigma/Aldrich, St. Louis, MO; 0 to 80 nM); the cells cultured with no peptides served as medium controls. To stimulate T cells from naïve mice, 96-well plates were coated with/without anti-CD3 (1.25 μg/ml) in the presence or absence of DHT (0 to 80 nM) or torin-1 (5 nM) (Cayman Chemical, Ann Arbor, MI) and their corresponding controls. Cells were plated at a density of 5×10^6 cells/ml in triplicates for 24 h in growth medium. After pulsing with tritiated ^{3}[H]-thymidine (1 μCi per well; MP Biomedicals,

Santa Ana, CA) for 16 h, proliferative responses were measured as counts per minute using a Wallac liquid scintillation counter (Perkin Elmer, Waltham, MA) (Massilamany et al. 2010; Massilamany et al. 2011b).

Annexin V/Propidium Iodide (PI) Staining

LNCs obtained from SJL mice immunized with PLP 139-151 were stimulated with or without PLP 139-151 or NASE 101-120 (0 to 80 μg/ml) and DHT (0 to 80 nM) or ethanol as described above. At 72 h, early apoptotic cells and late apoptotic (secondary necrosis) or necrotic cells were determined with annexin V and PI staining according to manufacturer's recommendations (eBioscience, San Diego, CA). Similarly, LNCs obtained from naïve mice were plated in 96-well plates coated with/without anti-CD3 (1.25 μg/ml) in the presence or absence of ethanol (vehicle) or DHT (40 nM). At 5 h and 10 h poststimulation, cells were stained with annexin V and PI, and the respective populations were then analyzed by flow cytometry. In experiments that involved the determination of cell death in cultures exposed to torin-1, cells were plated in 96- well plates coated with/without anti-CD3 (1.25 μg/ml) in the presence or absence of DHT (0 to 80 nM) or torin-1 (5 nM) (Cayman Chemical, Ann Arbor, MI) and their corresponding controls. After 24 h, cells positive for annexin V, and PI were determined. While, externalization of phosphatidylserine was detected by using annexin V conjugated with allophycocyanin (APC), PI uptake was used as a marker for loss of plasma membrane integrity. These analyses respectively permitted us to identify two cell populations: early apoptotic cells (annexin V^+, PI^-); and dead cells that included both necrotic and secondary necrotic (late apoptotic) cells (PI^+, annexin V^+).

Creation of IA^S Dextramers and Determination of Antigen Specificity by Dextramer Staining

To determine the frequency of antigen-specific T cells, IA^S/PLP 139-151 and Theiler's murine encephalomyelitis virus (TMEV) 70–86 dextramers were generated as described (Massilamany et al. 2011c). LNCs obtained from the mice immunized with PLP 139-151 were stimulated with PLP 139-151 for two days, and the cultures were then maintained in IL-2-medium (5 μM) (AB Biotechnologies, Columbia, MD). Viable lymphoblasts were harvested on day 5 poststimulation and stained at room temperature (RT) for 2 h with APC-conjugated IA^S dextramers (4.5 μg/ml) in IL-2-medium containing 2.5 % FBS, pH 7.63. After washing twice, cells were stained with anti-CD4 and 7-aminoactinomycin-D (7-AAD) (Invitrogen, Eugene, OR) and acquired by flow cytometer (FACS Calibur, BD Bioscience, San Diego, CA). The frequency of $dextramer^+$ ($dext^+$) cells was then enumerated in the live (7-AAD^-) $CD4^+$ subset using Flow Jo software (Tree Star, Ashland, OR).

Cytokine Analysis

Cytometric Bead Array Analysis

LNCs obtained from immunized mice were stimulated with or without PLP 139-151 (20 μg/ml) or DHT (40 nM) and their corresponding controls [medium alone, NASE 101-120 (control peptide) and ethanol (vehicle)]. Supernatants were harvested on day 3 poststimulation and analyzed for detection of cytokines using beads conjugated with capture antibodies, and phycoerythrin-conjugated detection antibodies for the indicated cytokines according to the manufacturer's recommendations (BD Bioscience). Briefly, to obtain standard curves, the combined mouse cytokine standards (representing Th1: IL-2 and interferon (IFN)-γ; Th2: IL-10; Th17: IL-17A; IL-6 and tumor necrosis factor (TNF)-α) were diluted serially (1:2) in 5-ml tubes that represent concentrations ranging from 20 to 5000 pg/ml, with the assay diluent alone serving as a 'zero' standard. In another tube, the capture beads (coated with capture antibodies) representing the above cytokines were mixed together, and 50 μl of this was added to 50 μl of the diluted standards or test samples. After adding the detection antibodies, the tubes were incubated at RT in the dark for 2 h. Both the standards and test samples were then centrifuged (200 g), and the pellets were washed. Finally, the pellets were resuspended in wash buffer, the beads were acquired by flow cytometry, and the data were analyzed by FCAP Array Software (BD Bioscience).

Intracellular Staining

LNCs obtained from the mice immunized with PLP 139-151 were restimulated with PLP 139- 151 for three days, and the cultures were then maintained in IL-2-medium. Viable lymphoblasts were harvested on day 5, and the cells were stimulated for 5 h with phorbol 12-myristate 13-acetate (PMA) (20 ng/ml) and ionomycin (300 ng/ml) (Sigma/Aldrich) in the presence of 2 mM monensin (Golgi stop, BD Bioscience). After staining with anti-CD4 and 7-AAD, cells were fixed, permeabilized and stained with cytokine antibodies or isotype controls (eBioscience). The frequency of cytokine-producing cells was then enumerated in the live (7- AAD^-) $CD4^+$ subset by flow cytometry using Flow Jo software (Reddy et al. 2004). The clones of cytokine antibodies used were: IL-2 (JES6-5H4), IL-4 (11B11), IL-6 (MP5-20F3), IL-10 (JES5-16E3), IL-17A (eBio 17B7), IFN-γ (XMG1.2), and TNF-α (MP6- XT22) (all from eBioscience).

To determine the frequencies of $dext^+$ cells in relation to cytokine-producing CD4 T cells, cells from different treatment groups harvested on day 6 poststimulation were stim-

ulated with PMA/ionomycin in the presence of monensin as described above. After washing, cells were stained with IA^S/dextramers (PLP 139-151 and TMEV 70-86) followed by anti-CD4 and 7-AAD. Cells were washed, fixed, and permeabilized, then stained with cytokine antibodies and their corresponding isotype controls. After the cells were acquired by flow cytometry, the percentages of dextramer$^+$ live (7-AAD$^-$) cytokine-producing CD4 T cells were enumerated using Flow Jo software (Massilamany et al. 2011c).

Western blotting Analysis

LNCs obtained from naïve SJL mice were plated in 6-well plates at a density of 5×10^6 cells/ml in growth medium, and the cells were stimulated with or without anti-CD3 and DHT (0 to 40 nM) or ethanol. After 24 h, cells were harvested and washed with 1 × PBS, and the pellets were lysed using radioimmunoprecipitation assay buffer containing protease and phosphatase inhibitors and 0.5 M EDTA solution (Thermo Scientific, Rockford, IL). In some experiments, chloroquine (CQ) (40 μM) was added four hours prior to harvesting the cells. Samples were briefly sonicated for up to 5 s, and after centrifugation, supernatants were harvested (Garcia-Garcia et al. 2013) and the protein concentrations measured by bicinchoninic acid assay (Thermo Scientific). Equal amounts of total protein samples were resolved by sodium dodecyl sulfate-polyacrylamide gel electrophoresis (SDSPAGE), and the proteins were transferred to polyvinylidene fluoride or nitrocellulose membranes. The membranes were first blocked for 2 h using tris-buffered saline (TBS) buffer containing 5 % milk powder or 3 % BSA and 0.1 % Tween-20, and then incubated with the appropriate primary antibodies at 4 °C overnight. Two panels of antibodies were used: 1) apoptosis: purified mouse anti-human poly(ADP-ribose) polymerase (PARP-1) (1:125, BD Bioscience), anti-rabbit cleaved caspase 3 (1:1000, Cell Signaling, Danvers, MA); and 2) autophagy: anti-rabbit Beclin-1 (1:1000, Cell Signaling), anti-rabbit p62 (1:5000, Abcam, Cambridge, MA), anti-rabbit phospho-mammalian target of rapamycin (pmTOR) (1:1000, Cell Signaling) and anti-rabbit microtubule- associated protein light chain 3 (LC3) B (1:1000, Sigma/Aldrich). The membranes were then washed thrice using TBS containing 0.1 % Tween-20, and incubated with horseradish peroxidase (HRP)-conjugated secondary antirabbit (1:5000, Florence, KY) or anti-mouse (1:5000, Cell Signaling) antibodies for one hour. After addition of enhanced chemiluminescence (ECL) substrate (GE Healthcare, Boston, MAor Thermo Scientific), the images were captured using the ChemiDoc XRS Imaging System (BIO-RAD, Richmond, CA) (Munoz-Gamez et al. 2009). The blots were then reprobed using anti-mouse β-actin (1:5000, Sigma/Aldrich)/ secondary, anti-mouse HRP antibody to verify for equal protein loading in each experiment. Finally, the densities corresponding to each protein were quantified using the ImageJ Program (National Institutes of Health, http://rsb.info.nih.gov/ij), and the ratios were then derived by dividing the densities of target proteins by the densities of β-actin.

Statistics

To ascertain the differences between groups with respect to proliferation assay, annexin/PI staining and Western blotting analyses, values were analyzed by student's *t*. $P \leq 0.05$ values were considered significant.

Results and Discussion

Previous reports indicate that DHT exerts its effects on autoreactive T cells by promoting immune deviation from a pro-inflammatory (Th1) toward an anti-inflammatory (Th2) environment (Dalal et al. 1997; Bebo et al. 1999; Du et al. 2001; Liva and Voskuhl 2001), but the antigen specificity of targeted T cells was unclear. In order to study the effects of sex steroids like androgens on PLP-specific T cells, we recently created IA^S/PLP 139-151 dextramers as novel tools, permitting us to ascertain the generation, expansion, and functionalities of antigen-sensitized T cells in various systems (Massilamany et al. 2011c; Gangaplara et al. 2012; Massilamany et al. 2014).

First, to determine the effects of DHT on antigen-sensitized T cells, we optimized the conditions using T cell proliferation assay. In brief, LNCs were prepared from mice immunized with PLP 139-151, and the cells were stimulated with or without specific (PLP 139-151) or control NASE-101–120 (0 to 80 μg/ml) in the presence or absence of DHT (0 to 80 nM) or ethanol. After two days, proliferative responses were measured as a function of DNA synthesis based on incorporation of ^{3}[H]-thymidine. Cells stimulated with PLP 139-151, with or without ethanol, showed similar levels of responses, but addition of DHT led to reduction in the responses dose dependently ($p \leq 0.001$) (Figure 1a). The responses induced with PLP 139-151 were specific because the control, NASE 101-120, which also binds IA^S/MHC class II allele (Nicholson et al. 1997) much like PLP 139-151 does, did not stimulate the cells (Figure 1a). However, when the background responses were compared for the cells exposed to DHT and ethanol, it was evident that the levels of ^{3}[H]-thymidine incorporated in the cells exposed to DHT were significantly reduced dose dependently ($p \leq 0.007$) (Figure 1b). Previous reports about the effects of testosterone derivatives were conflicting. While dihydroepiandrosterone was shown to reduce proliferative responses in myelin-basic protein-sensitized T cells, DHT appeared not to influence the responses in PLP-reactive T cells (Bebo et al. 1999; Du et al. 2001). In our hands, the finding that DHT affects the proliferative responses of T

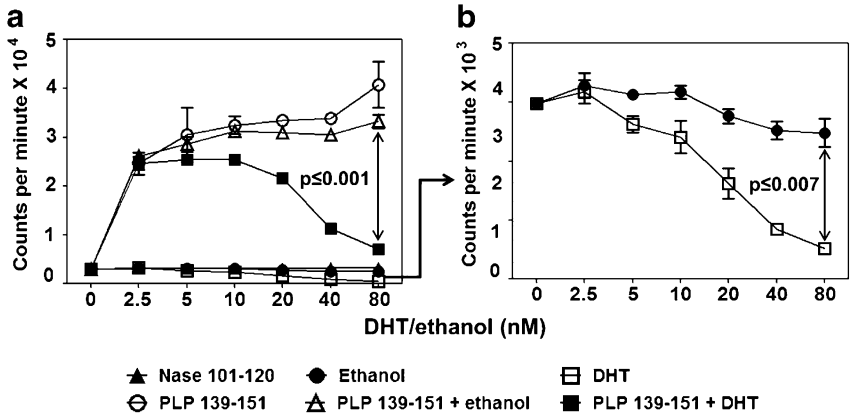

Figure 1. The inhibitory effect of DHT on T cell proliferation are not antigen-specific. SJL mice were immunized with PLP 139-151, and 10 days later, the animals were euthanized and the draining lymph nodes were harvested to prepare the single cell suspensions. Cells were stimulated with or without PLP 139-151/NASE 101-120 (control) (0 to 80 μg/ml) or DHT (0 to 80 nM)/ethanol (vehicle) for two days. After pulsing the cells with ^{3}[H]-thymidine for 16 h, proliferative responses were measured as counts per minute (panel, **a**). Panel (**b**) shows the blown up view of the effects of DHT on cells with no peptide stimulations in comparison with cells treated with ethanol alone. Mean ± SEM values obtained from three experiments each involving three mice are shown.

cells nonspecifically, independent of antigenic stimulation, was not expected, leading us to question whether DHT-mediated effects involve selective inhibition of antigen-specific T cells or nonspecific killing of T cells independent of their antigen specificity.

To address this question, we prepared two dextramers, one each for PLP 139-151 and TMEV 70-86. Both bind the IA^{S} allele, thus permitting us to use the TMEV 70-86 dextramer as the TCR-specificity control for PLP 139-151, as we have described previously (Massilamany et al. 2011c). Using these reagents, we analyzed the frequencies of antigen-specific T cells in cultures stimulated with PLP 139-151 in the presence or absence of DHT. In this setup, we used four controls that represent the cells cultured in medium alone, NASE 101-120, ethanol, and DHT alone. The data revealed the presence of PLP dext^{+} CD4 T cells in cultures stimulated with PLP 139-151, with or without ethanol, whereas in cultures stimulated in the presence of DHT, the PLP dext^{+} cells were significantly reduced by ~five-fold (3 % vs 0.6 %; Figure 2a and Figure 2b), suggesting that DHT might have selectively inhibited the expansion of PLP-specific cells. The dextramer staining was specific, since the control (TMEV 70-86) dextramer did not stain the cells in any of the above treatments. Likewise, none of the four control cell cultures (medium, NASE, ethanol, and DHT) stained with PLP 139-151 or TMEV 70-86 dextramers (Figure 2a and Figure 2b). Next, to determine whether failure to detect PLP dext^{+} cells in DHT-exposed PLP cultures is due to cell death induced by DHT, we stained the cells with 7-AAD to determine the percentages of live (7-AAD^{-}) and dead (7-AAD^{+}) cell populations by flow cytometry. Consistent with the patterns observed with the proliferative responses (Figure 1), the percentages of live cells were significantly reduced dose dependently in PLP 139-151-stimulated cultures exposed to DHT, when compared with cultures exposed to PLP 139-151 alone or PLP 139-151/ethanol (Figure 2c). More importantly, while the percentages of viable cells remained the same in cultures supplemented with the medium or ethanol, addition of DHT to cultures in the absence of PLP 139-151 also showed a reduction in the cell viability, compared to those exposed to ethanol (Figure 2c). Furthermore, to delineate the cell death pathway as it relates to early and late apoptosis/necrosis, we performed annexin V and PI staining to ascertain the respective cell populations in cultures stimulated with or without PLP 139-151 and DHT, and their corresponding controls. As shown in the Supplementary Table 1, cell viability followed the same pattern as that of 7-AAD^{+} cells (Figure 2c) dose-dependently in that the number of cells with compromised plasma membrane integrity (PI^{+}, annexin^{+}) were significantly increased in DHT-exposed cultures, whereas the apoptotic cells (annexin^{+}, PI^{-}) were reduced at higher doses (20 μM and above). These findings suggest possibly that early and late apoptosis/necrosis may occur continuously upon exposure to DHT. Similar results were noted when the cells were examined by annexin V/PI staining at early time points as well i.e., 24 and 48 h post-stimulation (data not shown). Overall, the findings that PLP dext^{+} cells were reduced in cultures stimulated with PLP 139-151/DHT (Figure 2a) and that DHT *per se* can kill the cells non-specifically (Figure 2c, Supplementary Table 1) led us to propose that DHT can affect both proliferating and nonproliferating cells.

In support of this proposition, we performed the experiments using LNCs from naïve mice, stimulating the cells with a polyclonal T cell activator, anti-CD3 (1.25 μg/ml), in the presence or absence of DHT or ethanol (Liva and Voskuhl 2001). By measuring the proliferative responses as shown with dose-response curves, it was evident that the responses were significantly reduced by 2- to 4-fold in cultures treated with DHT/anti-CD3 together when compared with those treated with the ethanol (Figure 3a). As noted above

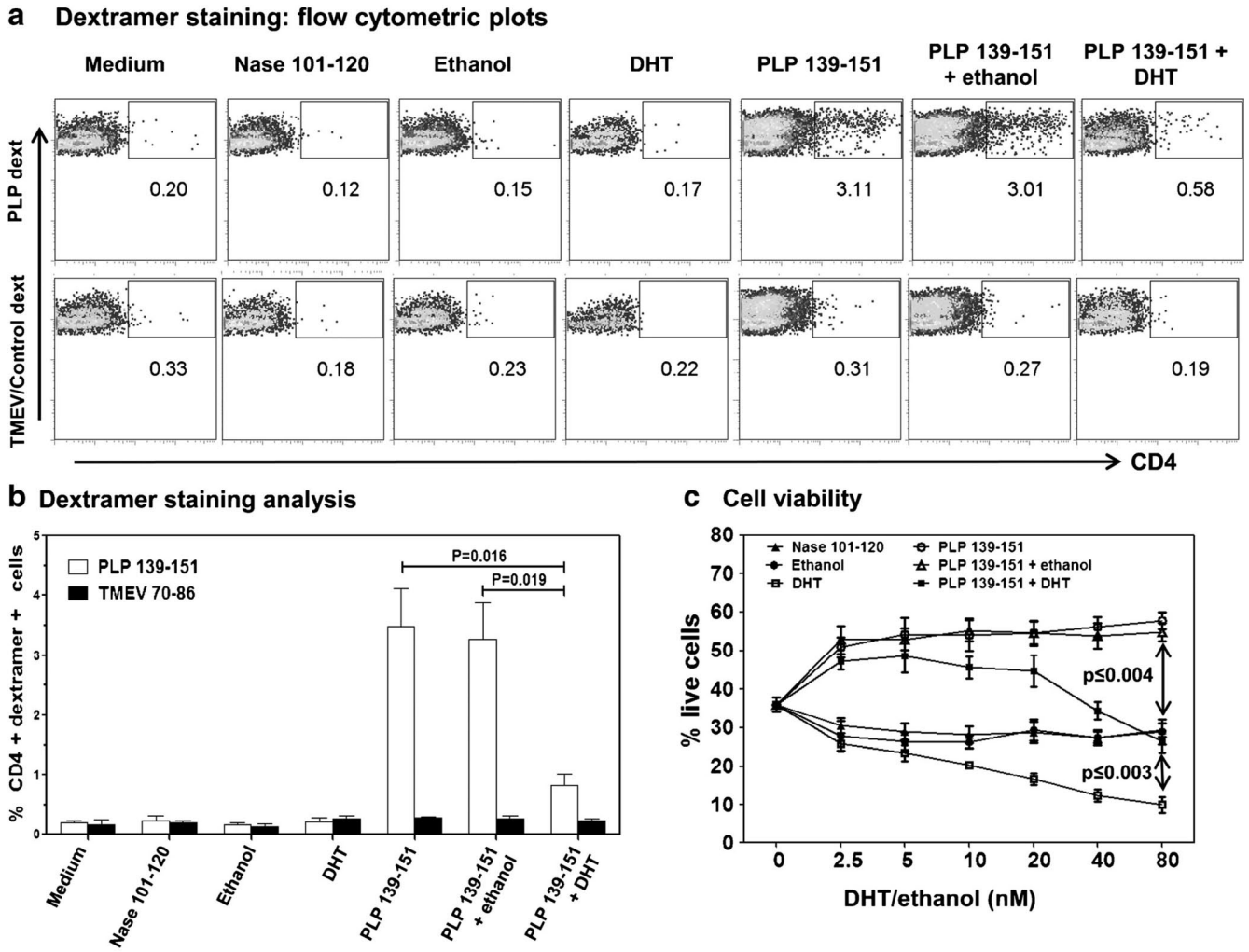

Figure 2. Frequencies of PLP 139-151-specific CD4 T cells are reduced in cultures exposed to DHT. **a.** Dextramer staining: flow cytometric plots. LNCs obtained from mice immunized with PLP 139-151 were stimulated with or without PLP 139-151/NASE 101-120 (control) (20 μg/ml) and DHT (40 nM)/ethanol. On day 3, the cultures were supplemented with IL- 2-medium (5 μM). Viable cells were harvested on day 5 poststimulation and stained with PLP 139-151/TMEV 70-86 (control) dextramers, anti-CD4, and 7-AAD. After washing and resuspending in 1xPBS/2.5%FBS, cells were acquired by flow cytometry. Percentages of dext$^+$ CD4$^+$ cells within the live (7-AAD$^-$) subset were then analyzed using Flow Jo software. **b.** Dextramers staining analysis. Mean ± SEM values representing the dext$^+$ CD4$^+$ cells obtained from four individual experiments each involving one mouse are shown. **c.** Cell viability. Antigen-sensitized LNCs prepared from the immunized animals were stimulated with or without PLP 139-151/NASE 101-120 (control) (0 to 80 μg/ml) or DHT (0 to 80 nM)/ethanol (vehicle) as above, and on day 3 poststimulation, cells were harvested and stained with 7-AAD. After acquiring the cells by flow cytometry, percentages of cells positive or negative for 7-AAD were then determined using Flow Jo software. Mean ± SEM values obtained from three experiments each involving three mice are shown.

(Figure 1b), the background responses in the naïve T cells exposed to DHT alone also were significantly reduced by 2- to 3-fold as compared to those treated with ethanol (Figure 3b). Since DHT showed similar responses regardless of the stimuli used (PLP 139-151: Figure 1 and Figure 2; or anti-CD3: Figure 3), we decided to use anti-CD3 for further experimentation to address the mechanistic basis for effects of DHT on T cells.

Previous reports indicated a skewed response from an IFN-γ-producing Th1 phenotype to an IL-10-producing Th2 phenotype in splenocytes/mixed T cell cultures treated with DHT (Bebo et al. 1999; Liva and Voskuhl 2001), but it was not clear whether T cells were the only source for IL-10, and if so, whether they were antigen specific. To address this question, we took the advantage of using PLP 139-151 dextramers to enumerate the frequencies of cytokine-producing, PLP specific CD4 T cells. Briefly, LNCs obtained from mice immunized with PLP 139-151 were stimulated with PLP 139- 151 or control (NASE 101-120) with or without DHT or its ethanol. First, we analyzed the cytokine secretion in culture supernatants on day 3 poststimulation using cytokine capture beads to include a panel of Th1, Th2, and Th17 cytokines, in addition to two other inflammatory cytokines, IL-6 and TNF-α (Wei et al. 2014). The data revealed that

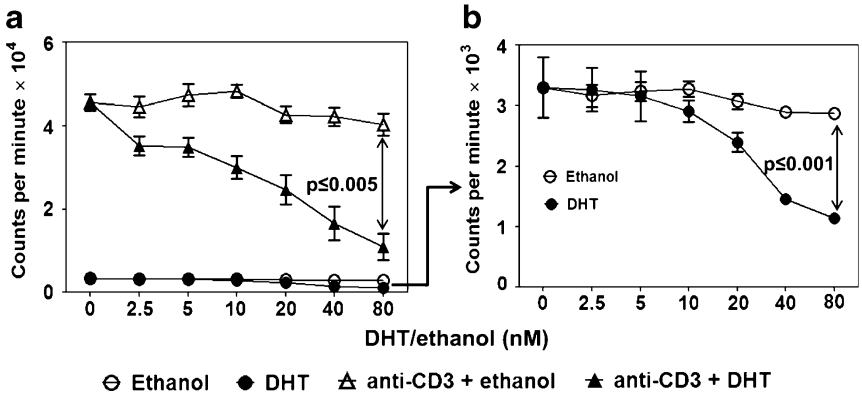

Figure 3. DHT mediates its effects on both proliferating and nonproliferating T cells. LNCs were prepared from naïve SJL mice, and the cells were stimulated with or without anti-CD3 (1.25 μg/ml) and DHT (0 to 80 nM)/ethanol. After 24 h, cells were pulsed with ^{3}[H]-thymidine, and 16 h later, proliferative responses were measured as counts per minute **a**. The blown-up view of the effects of DHT on cells with no anti-CD3-stimulation is shown in panel **b**. Mean ± SEM values obtained from three individual experiments each involving three mice per group are shown.

supernatants obtained from cells stimulated with PLP 139-151 with or without ethanol showed the presence of all the cytokines, in the order from Th1, followed by Th17 and Th2 cytokines, and TNF-α and IL-6 (Figure 4). Of note, non-antigen-specific IFN-γ production was noted in cells cultured in medium alone, ethanol or with NASE 101-120. However, in response to PLP 139-151 stimulation, IFN-γ production was increased (~2- fold), indicating that response was antigen-specific. Conversely, the amounts of cytokines, including IL-10, detected in culture supernatants from DHT/PLP 139-151- treated cells were significantly reduced. Likewise, background cytokine production in control cell cultures exposed to DHT was also significantly reduced (Figure 4).

We then sought to determine the frequencies of cytokine-producing CD4 T cells at a single cell level by intracellular staining through flow cytometry. The data revealed that the cultures derived from PLP 139-151 stimulation, with or without ethanol, showed predominantly the presence of Th1 cytokine (IFN-γ)-producing cells, followed by Th17 (IL-17A) (Table 1, and Supplementary Figure 1). In contrast, in DHT-treated cultures, frequencies of cells producing all the above cytokines were significantly reduced. While IL-4- and IL-10-producing cells in PLP-stimulated cultures were negligible, DHT-exposed cells did not show any shift in the cells producing these cytokines. While IL-6$^+$ cells were almost absent, the number of TNF-α-producing CD4 cells was unexpectedly greater in PLP-stimulated cultures that were exposed to DHT (Table 1, and Supplementary Figure 1). The background cytokine responses in control cultures (medium, NASE, ethanol or DHT) were negligible, except for IL-2, whose expression occurred non-specifically in all the cultures. Thus, the cytokine patterns as evaluated based on cytometric bead array analysis (Figure 4) and intracellular staining, complemented each other (Table 1, and Supplementary Figure 1). Overall, on one hand, these data seemed to conflict with previous reports due to the lack of shift towards the Th2 phenotype**;** on the other hand, a possibility existed that such a deviation might have occurred selectively in the non-antigen-specific T cells.

To address this possibility, we used IA^S/PLP 139-151 dextramers that permitted us to determine cytokine-producing, PLP-specific CD4 T cells in a multicolor flow cytometric analysis, leading us to obtain three data sets — dex$^-$cyt$^+$, dex$^+$cyt$^-$, and dex$^+$cyt$^+$ — for Th1, Th2, and Th17 cytokines and TNF-α (Table 2, and Supplementary Figure 2). All these analyses included the use of control (TMEV 70-86) dextramers to define the TCR specificity for PLP 139-151 dextramers, and isotype controls for cytokine antibodies, but their corresponding background staining intensities were negligible (Table 2, and Supplementary Figure 2). By tabulating the data for each cytokine, we noted that the majority of cytokine-producing cells did not stain with PLP dextramers, but a proportion of dextramer$^+$ cells also were positive for cytokines (Supplementary Figure 2). In cultures stimulated with PLP 139- 151 or PLP 139-151/ethanol, percentages of dext$^+$cyt$^+$ cells in relation to dext$^+$cyt$^-$ were found to be in the order of IFN-γ, followed by TNF-α, and IL-17A (Table 2). In contrast, subsets of dex$^+$IFN-γ$^+$ ($p = 0.002$) and dex$^+$ IL-17$^+$ ($p = 0.047$) cells in cultures stimulated with PLP 139-151 in the presence of DHT were significantly reduced when compared with cells cultured with PLP 139-151 in the presence of ethanol. Additionally, frequencies of cells belonging to two other subsets — dext$^-$cyt$^+$, and dext$^+$cyt$^-$ cells — also were significantly low in DHT-exposed cells (Table 2, and Supplementary Figure 2). More importantly, shift in the production of IL-4- and IL-10-producing cells, if any, was absent within the dextramer$^+$ cells (see dex$^+$ IL-4$^+$ and dex$^+$ IL-10$^+$ subsets in Table 2, and Supplementary Figure 2). On the contrary, the background cytokine responses with respect to IL-4 and IL-10 in DHT-exposed PLP 139-151-stimulated cultures were maintained, but were independent of DHT treatment, as the control cultures (cells in medium, NASE 101-120, ethanol alone or DHT alone) also had similar background levels for all the cytokines, including IL-4

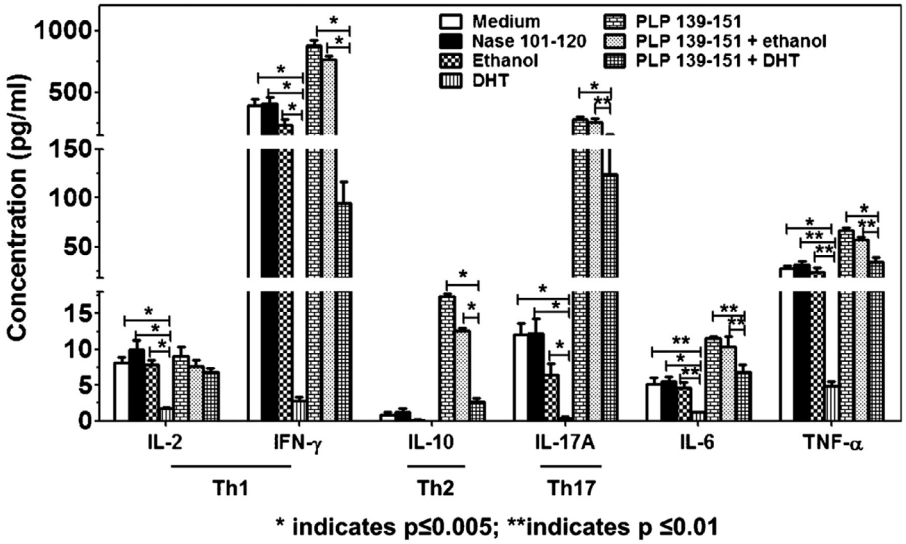

Figure 4. Th1 and Th17 cytokine responses are reduced, but with no skewed Th2 phenotype in cells exposed to DHT. LNCs obtained from PLP 139-151-immunized mice were stimulated with or without PLP 139-151/NASE 101-120 (control) (20 μg/ml) and DHT (40 nM)/ethanol. Supernatants were collected on day 3 poststimulation and analyzed using beads conjugated with capture antibodies for the indicated cytokines by cytometric bead array as described in the Methods section. Mean ± SEM values obtained from three individual experiments for each cytokine are shown, and their profiles are compared between treatment groups. Mean ± SEM values obtained from three experiments each involving three mice are shown.

and IL-10 (Table 2, and Supplementary Figure 2). Furthermore, it is to be noted that, in contrast to our observation that more TNF-α^+ cells were found to be in the whole CD4 T cell subset in DHT/PLP-treated cultures (Table 1), we did not observe such an effect at the antigen-specific T cell level, as the frequencies of dext$^+$ TNF-α^+ cells were not elevated under similar conditions (Table 2). Taking the analyses of cytometric bead arrays and intracellular cytokine/dextramer stainings together, the data suggest that DHT did not induce any deviation for any of the cytokines tested. On the contrary, reduction in the cytokine-producing cells in the DHT/PLP-139–151-treated cells might be the result of cell death induced by DHT.

Induction of cell death by DHT has been reported in various cell lines and primary immune cells such as macrophages and PBMCs (Bebo et al. 1998; Huber et al. 1999; McMurray et al. 2001; Cutolo et al. 2002; Ling et al. 2002; Verzola et al. 2004; Cutolo et al. 2005). In our studies that involve mouse primary T cells, we sought to determine whether DHT-mediated effects on cell viability can be differentiated with respect to early-stage or late-stage apoptotic/necrotic cells based on annexin V/PI staining. As shown in Supplementary Figure 3, annexin V/PI staining of cells stimulated with or without anti-CD3 at both 5 and 10 h poststimulation revealed increase in the cells with compromised plasma membrane integrity (PI$^+$, annexin$^+$), but not apoptotic cells

Table 1. Frequencies of cytokine-producing CD4 T cells in cultures stimulated with or without PLP 139-151 and DHT

Group	Percentages of cytokine+CD4+ T cells (Mean ± SEM)							
	Th1		Th2		Th17	Other inflammatory cytokines		
	IL-2	IFN-γ	IL-4	IL-10	IL-17A	IL-6	TNF-α	Isotype
Medium	15.0 ± 2.0	2.6 ± 0.3	0.4 ± 0.0	0.4 ± 0.1	0.4 ± 0.1	0.9 ± 0.6	75.7 ± 2.6	0.2 ± 0.1
NASE	14.8 ± 2.5	2.1 ± 0.5	0.2 ± 0.1	0.4 ± 0.2	0.3 ± 0.1	0.2 ± 0.0	78.9 ± 4.6	0.1 ± 0.0
Ethanol	14.9 ± 1.8	1.1 ± 0.1	0.4 ± 0.2	0.4 ± 0.1	0.3 ± 0.0	0.2 ± 0.1	79.7 ± 1.6	0.1 ± 0.0
DHT	9.0 ± 2.3	0.2 ± 0.1	0.3 ± 0.2	0.3 ± 0.1	0.2 ± 0.2	0	60.2 ± 6.2	0
PLP	10.6 ± 2.3	13.9 ± 1.9	0.8 ± 0.3	1.0 ± 0.3	3.6 ± 0.4	0.3 ± 0.1	49.3 ± 2	0.2 ± 0.0
PLP + ethanol	12.3 ± 1.9	13.8 ± 2.1	0.4 ± 0.2	1.0 ± 0.1	2.2 ± 0.4	0.3 ± 0.1	56. ± 2.4	0.2 ± 0.1
PLP + DHT	12.1 ± 0.3	1.2 ± 0.1	0.2 ± 0.1	0.5 ± 0.0	0.7 ± 0.1	0.2 ± 0.0	68.9 ± 2.3	0.1 ± 0.1
p value*		0.013			0.007		0.030	

* represent comparisons between PLP + DHT, and PLP + ethanol groups

Table 2. Frequencies of cytokine-producing, PLP 139-151 dextramer$^+$ T cells in cultures stimulated with or without PLP 139-151 and DHT

Group	Percentages of cytokine producing CD4$^+$ T cells in relation to PLP 139-151 dextramer$^+$ cells (mean ± SEM)																	
	IFN-γ			IL-4				IL-10			IL-17A			TNF-α			Isotype control	
	Dext$^-$ IFN$^+$	Dext$^+$ IFN$^-$	Dext$^+$ IFN$^+$	Dext$^-$ IL-4$^+$	Dext$^+$ IL-4$^-$	Dext$^+$ IL-4$^+$	Dext$^-$ IL-10$^+$	Dext$^+$ IL-10$^-$	Dext$^+$ IL-10$^+$	Dext$^-$ IL-17$^+$	Dext$^+$ IL-17$^-$	Dext$^+$ IL-17$^+$	Dext$^-$ TNF$^+$	Dext$^+$ TNF$^-$	Dext$^+$ TNF$^+$	Dext$^-$ con$^+$	Dext$^+$ con$^-$	Dext$^-$ con$^+$
Medium	4.4 ±1.9	0.2 ±0.1	0.1 ±0.1	0.4 ±0.0	0.1 ±0.1	0	0.4 ±0.2	0.1 ±0.1	0	0.6 ±0.2	0.2 ±0.1	0	31.4 ±5.6	0.1 ±0.1	0.1 ±0.0	0.1 ±0.0	0.3 ±0.1	0
NASE	4.4 ±2.2	0.1 ±0	0	0.4 ±0.2	0.1 ±0.0	0	0.3 ±0.1	0.1 ±0.0	0	0.5 ±0.2	0.1 ±0.0	0	37. ±7.2	0.1 ±0.1	0.2 ±0.1	0.1 ±0.0	0.3 ±0.2	0
Ethanol	2.7 ±1.1	0.1 ±0.0	0	0.2 ±0.1	0.1 ±0.0	0	0.1 ±0.0	0.1 ±0.0	0	0.6 ±0.2	0.1 ±0.0	0	31.4 ±5.1	0.1 ±0.1	0	0.1 ±0.0	0.1 ±0.0	0
DHT	0.2 ±0.0	0	0	0.3 ±0.1	0	0	0.2 ±0.0	0.1 ±0.0	0	0.4 ±0.1	0.1 ±0.0	0	23.8 ±5.5	0.1 ±0.0	0	0	0	0
PLP	13.3 ±2.4	1.4 ±0.1	0.5 ±0.1	0.4 ±0.1	1.6 ±0.2	0	0.4 ±0.1	1.8 ±0.3	0	6.7 ±0.6	1.5 ±0.2	0.1 ±0.0	22.1 ±4.7	1.1 ±0.3	0.5 ±0.1	0.2 ±0.1	0.2 ±0	0
PLP + ethanol	14.7 ±3.5	1.3 ±0.3	0.6 ±0.2	0.3 ±0.0	1.8 ±0.3	0	0.4 ±0.1	1.8 ±0.3	0	5.9 ±1.6	1.6 ±0.3	0.1 ±0.0	24.2 ±4.5	1.2 ±0.3	0.6 ±0.2	0.1 ±0.0	0.2 ±0.0	0
PLP + DHT	2.2 ±0.7	0.5 ±0.1	0.1 ±0.0	0.5 ±0.1	0.7 ±0.3	0	0.6 ±0.2	0.6 ±0.2	0	1.8 ±0.5	0.5 ±0.1	0	26.1 ±2.5	0.6 ±0.2	0.2 ±0.1	0.1 ±0.1	0.3 ±0.2	0
p value*	0.004	0.005	0.002		0.031			0.023		0.001	0.005	0.047		0.036				

* represent comparisons between PLP + DHT, and PLP + ethanol groups

(annexin$^+$, PI$^-$), suggesting that apoptosis leading to necrotic cell death may occur continuously upon exposure to DHT. We then examined the cell death using cleaved/activated caspase 3 that gets activated during apoptosis triggered by various intrinsic and extrinsic stimuli (Wyllie et al. 1980; McIlwain et al. 2013). Caspase 3 normally exists as an inactive proenzyme called procaspase 3 (32 kDa). Upon activation, procaspase 3 is first cleaved to yield two fragments (19 kDa and 12 kDa), and the larger of these (19 kDa) is then cleaved to produce another small fragment (17 kDa) (Pan and Berk 2007). Under some conditions, activated caspase 3 can yield an additional fragment (27 kDa) (Hershberger et al. 2002; Muro et al. 2005). Additionally, we used PARP-1 (113 kDa) as another marker for apoptosis, since PARP-1 can act as a substrate for executioner caspases (Gobeil et al. 2001; Yu et al. 2002; Chaitanya et al. 2010). For example, caspase 3 can cleave PARP-1 to yield two fragments, 89 kDa and 24 kDa (Chaitanya et al. 2010). Using these readouts, we evaluated the effects of DHT in LNCs obtained from naïve mice, stimulating the cells with or without anti-CD3 in the presence or absence of DHT. Protein lysates were prepared from cultures representing the above treatments, and the expression of caspase 3 and PARP-1 proteins were analyzed by Western blotting analysis. Figure 5 (top panel) shows the presence of baseline levels of procaspase 3 (32 kDa), as well as in two cleaved fragments (27 kDa and 17 kDa) in cells treated with or without anti-CD3, but their levels were significantly enhanced dose dependently in response to DHT (Figure 5a and b). Similar trends were noted with the 19 kDa-fragment in response to DHT exposure in both anti-CD3-stimulated and unstimulated cells (Figure 5c). As to PARP-1, while the full-length protein (113 kDa) was detected at comparable levels in cells treated with or without anti-CD3 or DHT, the cleaved PARP-1 (89 kDa) was elevated dose dependently in response to DHT (Figure 5d). Nonetheless, the intensity of the cleaved PARP-1 fragment 89 kDa was found to be marginally higher in untreated cells than in the cells treated with anti-CD3. This may be due to the possibility that the cleaved PARP-1 may degrade to yield additional small fragments in the stimulated cells (Chaitanya et al. 2010). Overall, the elevated proportions of the cleaved fragments of both caspase 3 and PARP-1 that occurred in response to DHT support our proposal that DHT-mediated effects in T cells involved, at least partially, apoptotic cell death.

It has been reported that autophagy has both pro-survival and pro-cell death roles in T cells (Li et al. 2006; Hubbard et al. 2010; Bizargity and Schroppel 2014). Furthermore, autophagy can control cell death induced by IFN-γ signaling in Th cells (Feng et al. 2008) and influence antigen-presentation functions. mTOR regulates cell growth and proliferation, and downregulation of mTOR activity has been shown to precede autophagy (Jung et al. 2010). Since the mTOR pathway prevents autophagy, and DHT promotes cell death as described above, we set out a hypothesis that

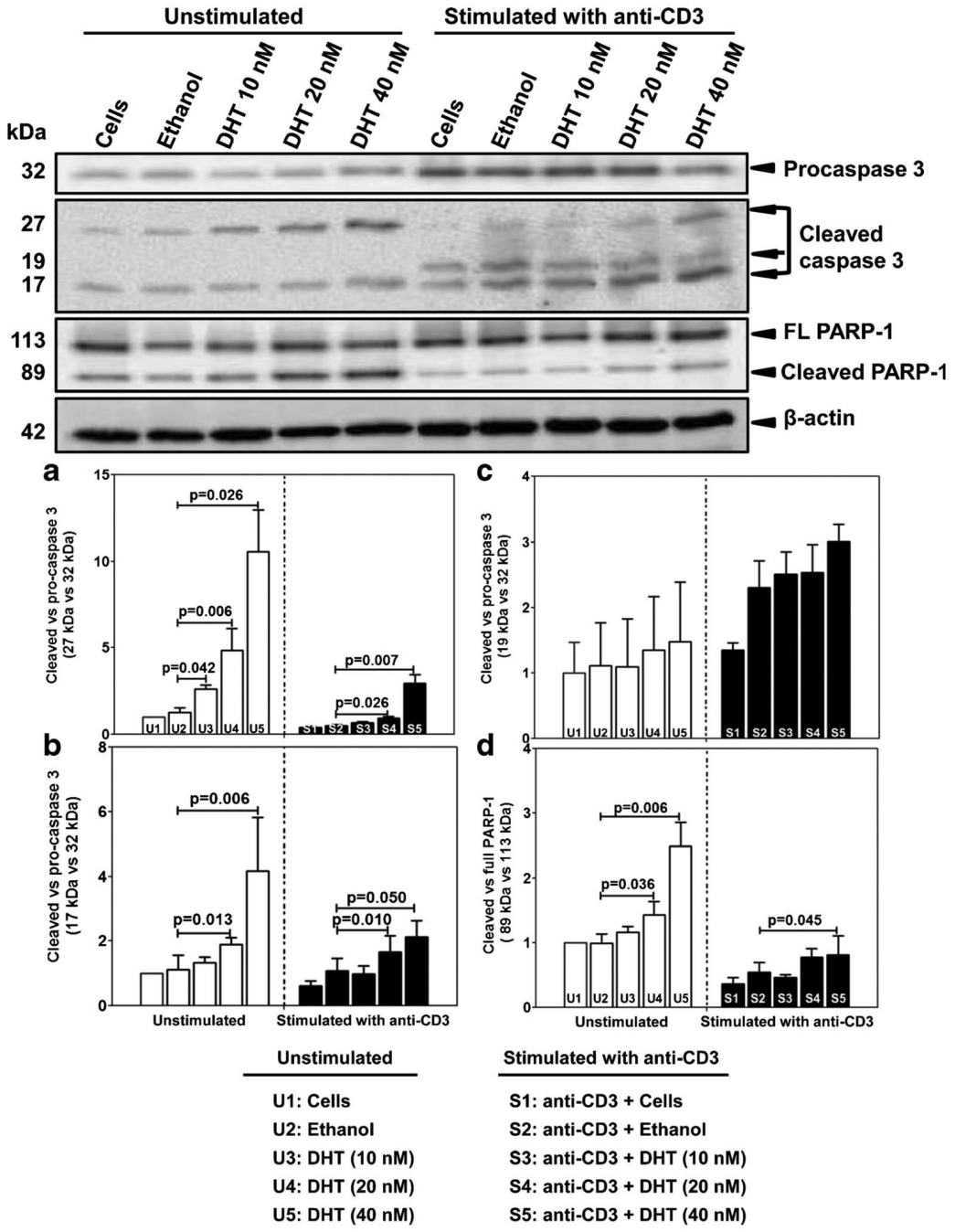

Figure 5. DHT triggers apoptotic pathway in cells stimulated with or without antigen. LNCs were obtained from naïve mice, and the cells were stimulated with or without anti-CD3 (1.25 μg/ml) and DHT (0 to 40 nM)/ethanol for 24 h. After centrifugation, cell pellets were lysed to obtain protein lysates, and equal amounts of proteins were resolved by SDS-PAGE analysis. The proteins were then transferred onto membranes stained with primary and HRP-conjugated secondary antibodies for the indicated molecules. After adding ECL substrate, the images were captured using Image system (top panel). β-actin, loading control (top panel). For quantification, the densities corresponding to the target proteins were measured, and the values were then normalized to β-actin-levels. To determine the change in the expression of cleaved caspase 3 (27 kDa, 19 kDa, and 17 kDa) in relation to procaspase 3 (32 kDa), the densities of each of the three cleaved caspase 3 bands were first normalized to procaspase 3. The density values corresponding to each set of bands (27 kDa/32 kDa; 19 kDa/32 kDa; and 17 kDa/32 kDa) were divided by the values for β-actin. Finally, the values obtained in cells cultured in medium alone were considered as 1 (baseline), to which expression levels in other treatment groups were compared. Similar analysis was performed for cleaved PARP-1, and the fold difference is shown in relation to full-length PARP-1. Mean ± SEM values obtained from three to six individual experiments each involving two to three mice per group are shown in the bottom panel: **a** cleaved caspase 3 (27 kDa) vs procaspase 3 (32 kDa); **b** cleaved caspase 3 (17 kDa) vs procaspase 3 (32 kDa); **c** cleaved caspase 3 (19 kDa) vs procaspase 3 (32 kDa); and **d** cleaved PARP-1 (89 kDa) vs PARP-1 (113 kDa).

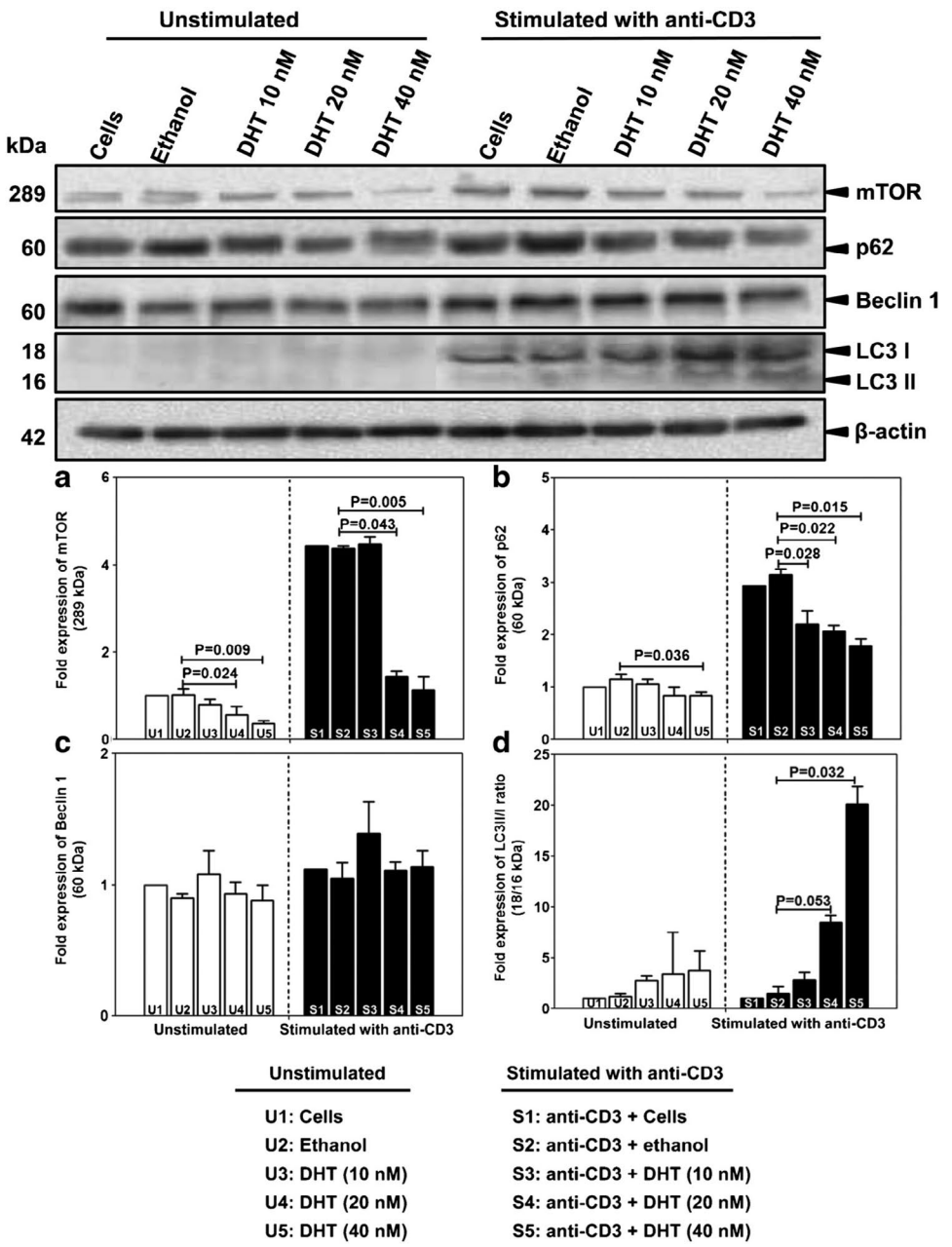

Figure 6. DHT triggers autophagy pathway in cells stimulated with or without antigenic stimulation. LNCs were obtained from naïve mice, and the cells were stimulated with or without anti-CD3 (1.25 μg/ml) and DHT (0 to 40 nM)/ethanol. After 24 h, cell pellets were lysed; proteins were resolved on SDS-PAGE analysis, and the transferred-proteins were probed with the indicated antibodies. The top panel shows the images for each protein, where β-actin was used as a loading control. The bottom panel indicates quantitative analysis to represent fold-change in the expression of target proteins (mTOR, p62, and Beclin 1) in relation to β-actin. For LC3 I and LC3 II, the density values for LC3 II (16 kDa) were divided by the density values for LC3 I (18 kDa), and the resulting values were then normalized to β-actin [(LC3 II/I)/ β-actin]. Finally, the values obtained in cells cultured in medium alone were considered as 1 (baseline), to which the values obtained in other treatment groups were compared. Mean ± SEM values obtained from three to six individual experiments each involving two to three mice per group are shown in the bottom panel: **a.** mTOR-expression; **b.** p62-expression; **c.** Belin 1-expression; and **d.** LC3 II/ LC3 I ratios.

DHT-induced cell death may involve the mediation of autophagy by downregulating the expression of mTOR. To test this hypothesis, we chose a panel of autophagy-related molecules: Beclin 1, LC3 I, LC3 II, and p62, in addition to mTOR. Beclin 1 acts as an upstream initiator of autophagy (Kang et al. 2011), while LC3 is a ubiquitin-like protein and in most circumstances is necessary for the formation of autophagosomes (Tanida et al. 2008; Choi et al. 2013). LC3 undergoes C-terminal cleavage generating a cytosolic LC3 I form that is conjugated to phosphatidylethanolamine on the autophagosomal membrane to form LC3 II (Tanida et al. 2008; Choi et al. 2013). As such, alterations in the levels of LC3 II, which migrates faster in SDS-PAGE compared to LC3 I, represent increased build-up of autophagosomes (Barth et al. 2010). Selective degradation of ubiquitinated protein aggregates by autophagy is mediated via the ubiquitin binding receptor, p62 (Ichimura and Komatsu 2010; Viiri et al. 2010). Thus, Beclin, LC3, and p62 are commonly used as markers of autophagy. By analyzing the expression of these molecules in cultures treated with or without anti-CD3/DHT by Western blotting analysis, we made two observations. (1) In unstimulated cells, while the level of Beclin 1 remained largely unchanged in response to DHT-supplementation, mTOR-expression was reduced with the increased concentrations of DHT ($p \leq 0.024$) (Figure 6a). In addition, expression of p62 also was reduced but only at high dose of DHT ($p = 0.036$) (Figure 6b). Conversely, LC3 I and LC3 II were not detected. (2) In cells stimulated with anti- CD3, although expression levels of p62 and Beclin 1 were found elevated in relation to unstimulated cells, DHT treatment reduced the expression

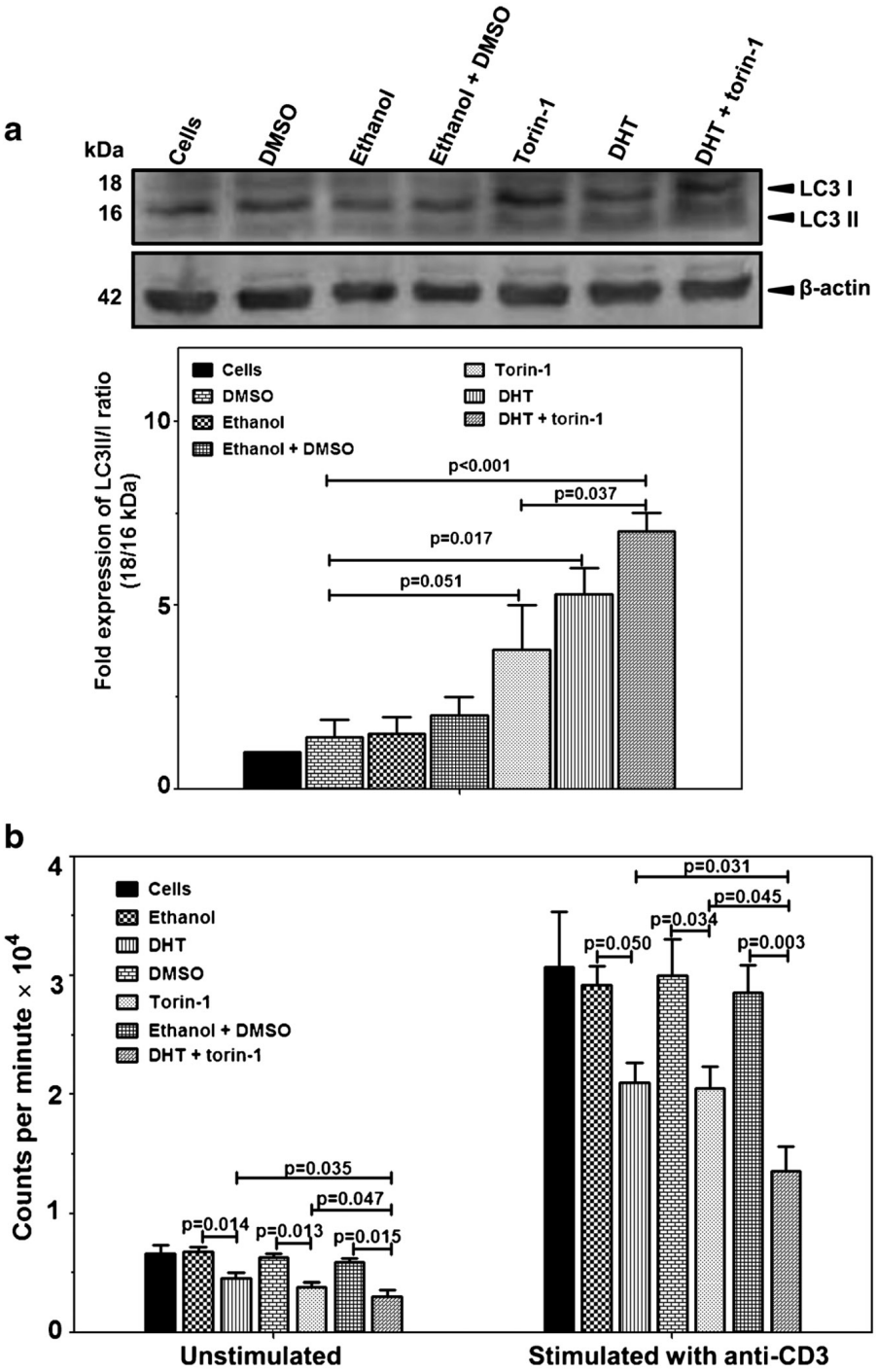

Figure 7. Evaluation of autophagy in cells treated with DHT in the presence of torin-1. **a.** Western blotting analysis. LNCs/splenocytes obtained from naïve mice were stimulated with anti-CD3 (1.25 μg/ml) in the presence or absence of ethanol (vehicle) or DHT (40 nM) for 24 h, and during the last eight hours, torin-1 (5 nM) or DMSO (vehicle) was added. Lysates prepared from the above treatments were subjected for SDS-PAGE analysis, and the transferred-proteins were probed with the antibody for LC3 I and LC3 II, where β-actin was used as a loading control. The top panel shows the image obtained by Western blotting analysis. The bottom panel represents quantitative analysis to depict fold-change in the expression of LC3 I and LC3 II proteins. The density values for LC3 II (16 kDa) were divided by the density values for LC3 I (18 kDa), and the resulting values were then normalized to β-actin [(LC3 II/I)/β-actin]. Finally, the values obtained in cells cultured in medium alone were considered as 1 (baseline), to which the values obtained in other treatment groups were compared. Mean ± SEM values obtained from three individual experiments each involving two mice are shown. **b.** Proliferation assay. LNCs obtained from naïve mice were stimulated with torin-1/DMSO (vehicle) (5 nM) for 24 h, with or without anti-CD3 (1.25 μg/ml) and DHT(10 nM)/ethanol. After pulsing with ^{3}[H]-thymidine for 16 h, proliferative responses were measured as counts per minute. Mean ± SEM values obtained from three experiments each involving three mice per group are shown.

of p62 ($p \leq 0.028$) (Figure 6b and c). While mTOR-expression was significantly reduced with increased concentrations of DHT, the appearance of LC3 proteins was apparent in the stimulated cultures (Figure 6d). Importantly, with an increased dose of DHT (0 to 40 nM), the ratios between LC3 II and LC3 I were proportionately increased (Figure 6: top right panel and Figure 6d). Furthermore, by using CQ as a blocker of autophagy to study autophagy flux, we noted an increase in LC3 II/LC3I ratios in the cells treated with DHT in the presence of CQ as compared to cells treated with ethanol and CQ, indicating increased autophagy induction (Supplementary Figure 4). The occurrence of reduced expression of mTOR corresponding to enhanced LC3 II/LC3 I ratios in cells exposed to DHT, but not in cells cultured in medium or ethanol alone, suggests that autophagy may possibly contributed to the effects mediated by DHT. To evaluate this possibility, we tested a hypothesis that torin-1, a known autophagy-inducer potentiates the effects of DHT in T cell proliferation assay (Peterson et al. 2011). First, we verified that torin-1 induces autophagy in T cells by evaluating the levels of LC3 I and LC3 II proteins as the prototypic marker for autophagy by Western blotting analysis. As shown in Figure 7a, torin-1-exposure to cells stimulated with anti-CD3 led to increase in LC3 II/LC3 I ratios indicating that torin-1 triggers autophagy in primary T cells. Second, supplementation of torin-1 to DHT-exposed cells also enhanced the ratios between LC3 II and LC3 I suggesting an additive effect between the two. We then stimulated LNCs obtained from naïve mice with or without anti-CD3/DHT or torin-1 and their corresponding controls (ethanol and DMSO). The data presented in Figure 7b indicate that cells treated individually with DHT ($p = 0.050$) or torin-1 ($p = 0.034$) showed a reduction in the proliferative responses to anti-CD3, but when both reagents were mixed, the responses were further reduced ($p = 0.003$), indicating the additive effects of both DHT and torin-1 together. The effects were specific, because the corresponding vehicles (ethanol for DHT or DMSO for torin-1)-treated cells did not affect the proliferative responses. Similar outcomes also were noted in unstimulated cells (Figure 7b). Under similar conditions, by verifying the cell death pathway, we noted that the cells double positive for PI and annexin were higher in cultures exposed to both DHT and torin-1 than their corresponding control (ethanol and DMSO), whereas the proportion of apoptotic cells remained the same (Supplementary Table 2). These results were expected, as DHT can induce cell death in both proliferating and non-proliferating cells as shown above (Figure 1, and Figure 3). The finding that DHT-induced cell death was accompanied by the occurrence of autophagy points to the possibility that autophagy-associated cell death may be one important mechanism by which DHT modulates the functions of autoreactive T cells.

In summary, we have demonstrated that DHT mediates its effects on T cells, but in a non-antigen-specific manner, leading us to make two key observations. (1) Mechanistically, cell death induced by DHT was associated with autophagy, suggesting that both processes might occur simultaneously. (2) Contrary to previous reports, using MHC class II dextramers we noted that immune deviation from the Th1 to Th2 phenotype was not evident in DHT-exposed antigen-specific T cells. Rather, frequencies of cytokine-producing, antigen-specific T cells were significantly reduced regardless of Th phenotype (Th1, Th2, or Th17). Previous reports indicate that DHT can ameliorate EAE when administered either during induction or in the effector phase of the disease process (Dalal et al. 1997; Bebo et al. 1999). Our observation that DHT induces cell death of both proliferating and non-proliferating naïve T cells may mean that the DHT-mediated effects might have occurred due to cell death. Likewise, although our data do not support the notion that DHT-mediated effects accompany the appearance of IL-10-producing cells (Dalal et al. 1997; Bebo et al. 1999; Liva and Voskuhl 2001), production of IL-10 by non-T cell sources in *in vivo* or mixed T cell cultures, in response to DHT-treatment cannot be discounted. Of note, the levels of DHT (active form of testosterone) are reported to be in the range of 0.47 to 2.65 nM/L in healthy adult men (Shiraishi et al. 2008). In our *in vitro* studies, we have seen the effects of DHT dose-dependently up to 40 nM as the equivalent amounts of vehicle (ethanol) did not induce any non-specific effects. Although, it is difficult to extrapolate the significance of *in vitro* data to the *in vivo* settings, we believe that the effects induced by DHT up to 40 nM may represent the supraphysiological or therapeutic dose. Our data support the notion that autophagy-associated cell death may contribute to DHT-mediated cell death. In the future, delineating the exact interrelationship between cell death and autophagy may possibly provide opportunities to target these pathways for therapy with DHT.

Acknowledgments — This work was in part supported by the National Institutes of Health (HL114669). TJ is a recipient of the China Scholarship Council Award.

Compliance with Ethical Standards — All applicable international, national, and/or institutional guidelines for the care and use of animals were followed. All procedures performed in studies involving animals were in accordance with the ethical standards of the University of Nebraska- Lincoln, Lincoln, NE, USA.

Conflict of Interest — The authors declare that they have no conflict of interest.

References

Barth S, Glick D, Macleod KF (2010) Autophagy: assays and artifacts. J Pathol 221:117–124

Bebo Jr BF, Schuster JC, Vandenbark AA, Offner H (1999) Androgens alter the cytokine profile and reduce encephalitogenicity of myelinreactive T cells. J Immunol (Baltimore, Md: 1950) 162:35–40

Bebo Jr BF, Vandenbark AA, Offner H (1996) Male SJL mice do not relapse after induction of EAE with PLP 139-151. J Neurosci Res 45:680–689

Bebo Jr BF, Zelinka-Vincent E, Adamus G, Amundson D, Vandenbark AA, Offner H (1998) Gonadal hormones influence the immune response to PLP 139-151 and the clinical course of relapsing experimental autoimmune encephalomyelitis. J Neuroimmunol 84:122– 130

Benten WP, Becker A, Schmitt-Wrede HP, Wunderlich F (2002) Developmental regulation of intracellular and surface androgen receptors in T cells. Steroids 67:925–931

Benten WP, Lieberherr M, Giese G, Wrehlke C, Stamm O, Sekeris CE, Mossmann H, Wunderlich F (1999) Functional testosterone receptors in plasma membranes of T cells. FASEB J : Off Publ Fed Am Soc Exp Biol 13:123–133

Bizargity P, Schroppel B (2014) Autophagy: Basic principles and relevance to transplant immunity. Am J Transplant : Off J Am Soc Transplant and the Am Soc Transpl Surg 14:1731–1739

Chaitanya GV, Steven AJ, Babu PP (2010) PARP-1 cleavage fragments: Signatures of cell-death proteases in neurodegeneration. Cell Commun Signal : CCS 8:31

Choi AM, Ryter SW, Levine B (2013) Autophagy in human health and disease. N Engl J Med 368:651–662

Compston A, McDonald I, Noseworthy J, Lassmann H, Miller D, Smith K, Wekerle H, Confavreux C (2006) McAlpine's multiple sclerosis, 4th ed. Churchill Livingstone Elsevier, Philadelphia

Confavreux C, Hutchinson M, Hours MM, Cortinovis-Tourniaire P, Moreau T (1998) Rate of pregnancy-related relapse in multiple sclerosis. Pregnancy Mult Scler Group N Engl J Med 339:285–291

Constantinescu CS, Farooqi N, O'Brien K, Gran B (2011) Experimental autoimmune encephalomyelitis (EAE) as a model for multiple sclerosis (MS). Br J Pharmacol 164:1079–1106

Cutolo M, Capellino S, Montagna P, Ghiorzo P, Sulli A, Villaggio B (2005) Sex hormone modulation of cell growth and apoptosis of the human monocytic/macrophage cell line. Arthritis Res Ther 7: R1124-R1132

Cutolo M, Sulli A, Craviotto C, Felli L, Pizzorni C, Seriolo B, Villaggio B (2002)Modulation of cell growth and apoptosis by sex hormones in cultured monocytic THP-1 cells. Ann NY Acad Sci 966:204–210

Dalal M, Kim S, Voskuhl RR (1997) Testosterone therapy ameliorates experimental autoimmune encephalomyelitis and induces a T helper 2 bias in the autoantigen-specific T lymphocyte response. J Immunol 159:3–6

Du C, Khalil MW, Sriram S (2001) Administration of dehydroepiandrosterone suppresses experimental allergic encephalomyelitis in SJL/J mice. J Immunol (Baltimore, Md : 1950) 167:7094–7101

Feng CG, Zheng L, Jankovic D, Bafica A, Cannons JL, Watford WT, Chaussabel D, Hieny S, Caspar P, Schwartzberg PL, Lenardo MJ, Sher A (2008) The immunity-related GTPase Irgm1 promotes the expansion of activated $CD4^+$ T cell populations by preventing interferon-gamma-induced cell death. Nat Immunol 9:1279–1287

Gangaplara A, Massilamany C, Brown DM, Delhon G, Pattnaik AK, Chapman N, Rose N, Steffen D, Reddy J (2012) Coxsackievirus B3 infection leads to the generation of cardiac myosin heavy chain-alpha-reactive CD4 T cells in A/J mice. Clin Immunol (Orlando, Fla) 144:237–249

Garcia-Garcia A, Anandhan A, Burns M, Chen H, Zhou Y, Franco R (2013) Impairment of Atg5-dependent autophagic flux promotes paraquat- and MPP(+)-induced apoptosis but not rotenone or 6-hydroxydopamine toxicity. Toxicol Sci: Off J Soc Toxicol 136: 166–182

Gobeil S, Boucher CC, Nadeau D, Poirier GG (2001) Characterization of the necrotic cleavage of poly(ADP-ribose) polymerase (PARP-1): Implication of lysosomal proteases. Cell Death Differ 8:588–594

Haegert DG, Marrosu MG (1994) Genetic susceptibility to multiple sclerosis. Ann Neurol 36:S204–S210

Hershberger PA, McGuire TF, Yu WD, Zuhowski EG, Schellens JH, Egorin MJ, Trump DL, Johnson CS (2002) Cisplatin potentiates 1, 25-dihydroxyvitamin D3-induced apoptosis in association with increased mitogen-activated protein kinase kinase kinase 1 (MEKK-1) expression. Mol Cancer Ther 1:821–829

Hubbard VM, Valdor R, Patel B, Singh R, Cuervo AM, Macian F (2010) Macroautophagy regulates energy metabolism during effector T cell activation. J Immunol (Baltimore, Md : 1950) 185:7349–7357

Huber SA, Kupperman J, Newell MK (1999) Estradiol prevents and testosterone promotes Fas-dependent apoptosis in $CD4^+$ Th2 cells by altering Bcl 2 expression. Lupus 8:384–387

Ichimura Y, Komatsu M (2010) Selective degradation of p62 by autophagy. Semin Immunopathol 32:431–436

Jung CH, Ro S-H, Cao J, Otto NM, Kim D-H (2010) MTOR regulation of autophagy. FEBS Lett 584:1287–1295

Kang R, Zeh HJ, Lotze MT, Tang D (2011) The beclin 1 network regulates autophagy and apoptosis. Cell Death Differ 18:571–580

Kovacs WJ, Olsen NJ (1987) Androgen receptors in human thymocytes. J Immunol (Baltimore, Md : 1950) 139:490–493

Li C, Capan E, Zhao Y, Zhao J, Stolz D, Watkins SC, Jin S, Lu B (2006) Autophagy is induced in $CD4^+$ T cells and important for the growth factor-withdrawal cell death. J Immunol (Baltimore, Md : 1950) 177:5163–5168

Ling S, Dai A, Williams MR, Myles K, Dilley RJ, Komesaroff PA, Sudhir K (2002) Testosterone (T) enhances apoptosis-related damage in human vascular endothelial cells. Endocrinology 143:1119–1125

Liva SM, Voskuhl RR (2001) Testosterone acts directly on $CD4^+$ T lymphocytes to increase IL-10 production. J Immunol (Baltimore, Md : 1950) 167:2060–2067

Massilamany C, Thulasingam S, Steffen D, Reddy J (2011b) Gender differences in CNS autoimmunity induced by mimicry epitope for PLP 139-151 in SJL mice. J Neuroimmunol 230:95–104

Massilamany C, Upadhyaya B, Gangaplara A, Kuszynski C, Reddy J (2011c) Detection of autoreactive CD4 T cells using major histocompatibility complex class II dextramers. BMC Immunol 12:40

Massilamany C, Gangaplara A, Jia T, Elowsky C, Kang G, Riethoven JJ, Li Q, Zhou Y, Reddy J (2014) Direct staining with major histocompatibility complex class II dextramers permits detection of antigenspecific, autoreactive CD4 T cells in situ. PLoS One 9:e87519

Massilamany C, Gangaplara A, Steffen D, Reddy J (2011a) Identification of novel mimicry epitopes for cardiacmyosin heavy chain-alpha that induce autoimmune myocarditis in a/J mice. Cell Immunol 271: 438–449

Massilamany C, Steffen D, Reddy J (2010) An epitope from *Acanthamoeba castellanii* that cross-react with proteolipid protein 139–151-reactive T cells induces autoimmune encephalomyelitis in SJL mice. J Neuroimmunol 219:17–24

McCarthy DP, Richards MH, Miller SD (2012) Mouse models of multiple sclerosis: experimental autoimmune encephalomyelitis and Theiler's virus-induced demyelinating disease. Methods Mol Biol (Clifton, NJ) 900:381–401

McIlwain DR, Berger T, Mak TW (2013) Caspase functions in cell death and disease. Cold Spring Harb Perspect Biol 5:a008656

McMurray RW, Suwannaroj S, Ndebele K, Jenkins JK (2001) Differential effects of sex steroids on T and B cells: Modulation of cell cycle phase distribution, apoptosis and bcl-2 protein levels. Pathobiol : J Immunol, Mol Cell Biol 69:44–58

Miller SD, Karpus WJ, Davidson TS (2007) Experimental autoimmune encephalomyelitis in the mouse. Curr Protoc Immunol 4:15.11. 11– 15.11. 20.

Munoz-Gamez JA, Rodriguez-Vargas JM, Quiles-Perez R, Aguilar-Quesada R, Martin-Oliva D, de Murcia G, Menissier de Murcia J, Almendros A, Ruiz de Almodovar M, Oliver FJ (2009) PARP-1 is involved in autophagy induced by DNA damage. Autophagy 5:61–74

Muro I, Means JC, Clem RJ (2005) Cleavage of the apoptosis inhibitor DIAP1 by the apical caspase DRONC in both normal and apoptotic drosophila cells. J Biol Chem 280:18683–18688

Nicholson LB, Murtaza A, Hafler BP, Sette A, Kuchroo VK (1997) A T cell receptor antagonist peptide induces T cells that mediate bystander suppression and prevent autoimmune encephalomyelitis induced with multiple myelin antigens. Proc Natl Acad Sci USA 94:9279–9284

Palaszynski KM, Loo KK, Ashouri JF, Liu HB, Voskuhl RR (2004) Androgens are protective in experimental autoimmune encephalomyelitis: Implications for multiple sclerosis. J Neuroimmunol 146: 144–152

Pan S, Berk BC (2007) Glutathiolation regulates tumor necrosis factor-alpha-induced caspase-3 cleavage and apoptosis: Key role for glutaredoxin in the death pathway. Circ Res 100:213–219

Peterson TR, Sengupta SS, Harris TE, Carmack AE, Kang SA, Balderas E, Guertin DA, Madden KL, Carpenter AE, Finck BN, Sabatini DM (2011) MTOR complex 1 regulates lipin 1 localization to control the SREBP pathway. Cell 146:408–420

Reddy J, Illes Z, Zhang X, Encinas J, Pyrdol J, Nicholson L, Sobel RA, Wucherpfennig KW, Kuchroo VK (2004) Myelin proteolipid protein-specific $CD4^+$ $CD25^+$ regulatory cells mediate genetic resistance to experimental autoimmune encephalomyelitis. Proc Natl Acad Sci USA 101:15434–15439

Shiraishi S, Lee PW, Leung A, Goh VH, Swerdloff RS, Wang C (2008) Simultaneous measurement of serum testosterone and dihydrotestosterone by liquid chromatography-tandem mass spectrometry. Clin Chem 54:1855–1863

Soldan SS, Alvarez Retuerto AI, Sicotte NL, Voskuhl RR (2003) Immune modulation in multiple sclerosis patients treated with the pregnancy hormone estriol. J Immunol (Baltimore: 1950) 171:6267–6274

Tanida I, Ueno T, Kominami E (2008) LC3 and Autophagy. Methods Mol Biol (Clifton, NJ) 445:77–88

Verzola D, Gandolfo MT, Salvatore F, Villaggio B, Gianiorio F, Traverso P, Deferrari G, Garibotto G (2004) Testosterone promotes apoptotic damage in human renal tubular cells. Kidney Int 65:1252–1261

Viiri J, Hyttinen JM, Ryhanen T, Rilla K, Paimela T, Kuusisto E, Siitonen A, Urtti A, Salminen A, Kaarniranta K (2010) p62/sequestosome 1 as a regulator of proteasome inhibitor-induced autophagy in human retinal pigment epithelial cells. Mol Vis 16:1399–1414

Wei H, Tan K, Sun R, Yin L, Zhang J, Pu Y (2014) Aberrant production of Th1/Th2/Th17-related cytokines in serum of C57BL/6 mice after short-term formaldehyde exposure. Int J Environ Res Public Health 11:10036–10050

Wyllie AH, Kerr JR, Currie A (1980) Cell death: The significance of apoptosis. Int Rev Cytol 68:251–306

Yu SW, Wang H, Poitras MF, Coombs C, Bowers WJ, Federoff HJ, Poirier GG, Dawson TM, Dawson VL (2002) Mediation of poly(ADP-ribose) polymerase-1-dependent cell death by apoptosis-inducing factor. Science (New York) 297: 259–263

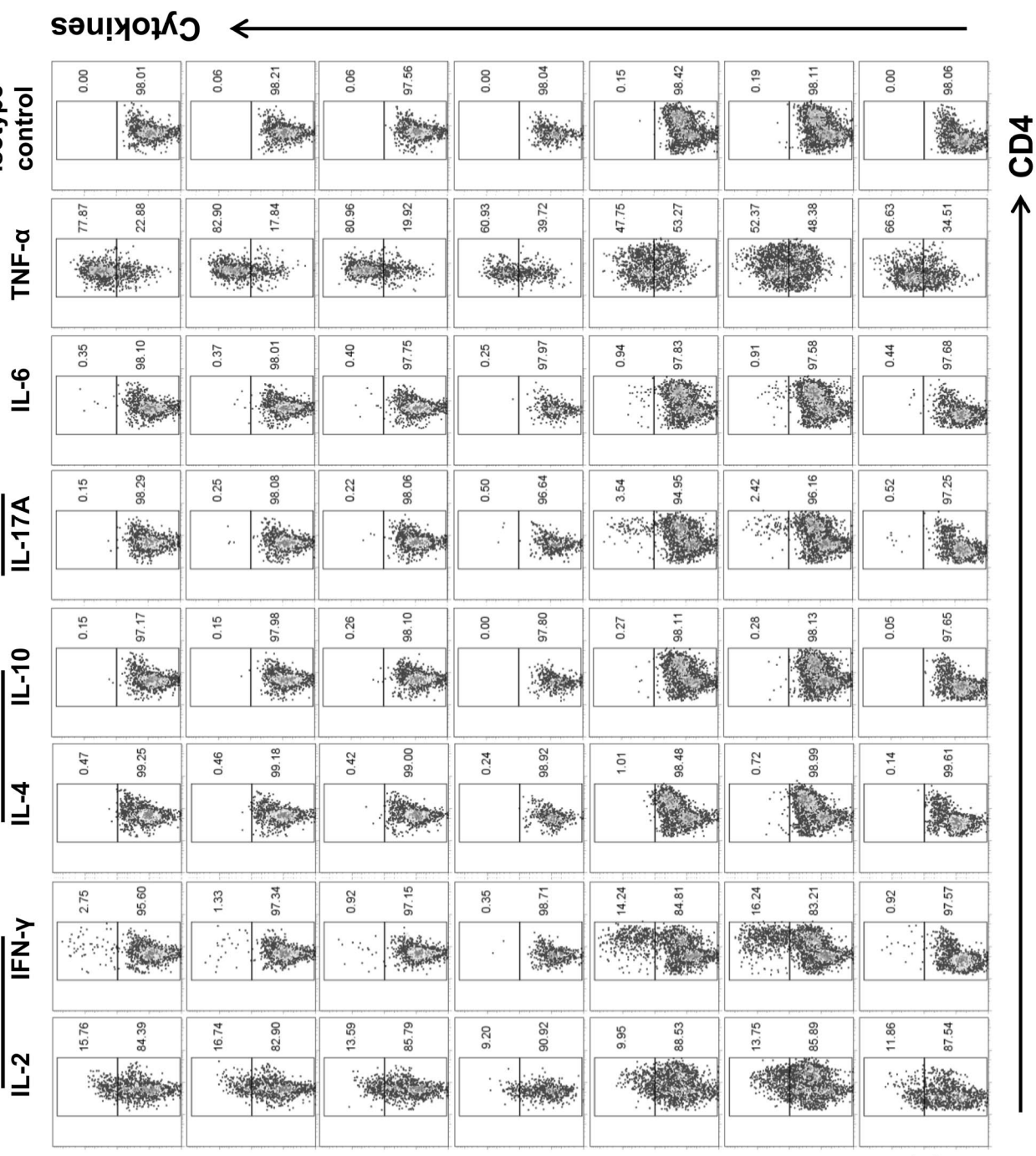
Treatment
Th1
IL-2
IFN-γ
Th2
IL-4
IL-10
Th17
IL-17A
IL-6
TNF-α
Isotype control
Cytokines
CD4
Medium
Nase 101-120
Ethanol
DHT
PLP 139-151
PLP 139-151 + ethanol
PLP 139-151 + DHT

S Fig. 1

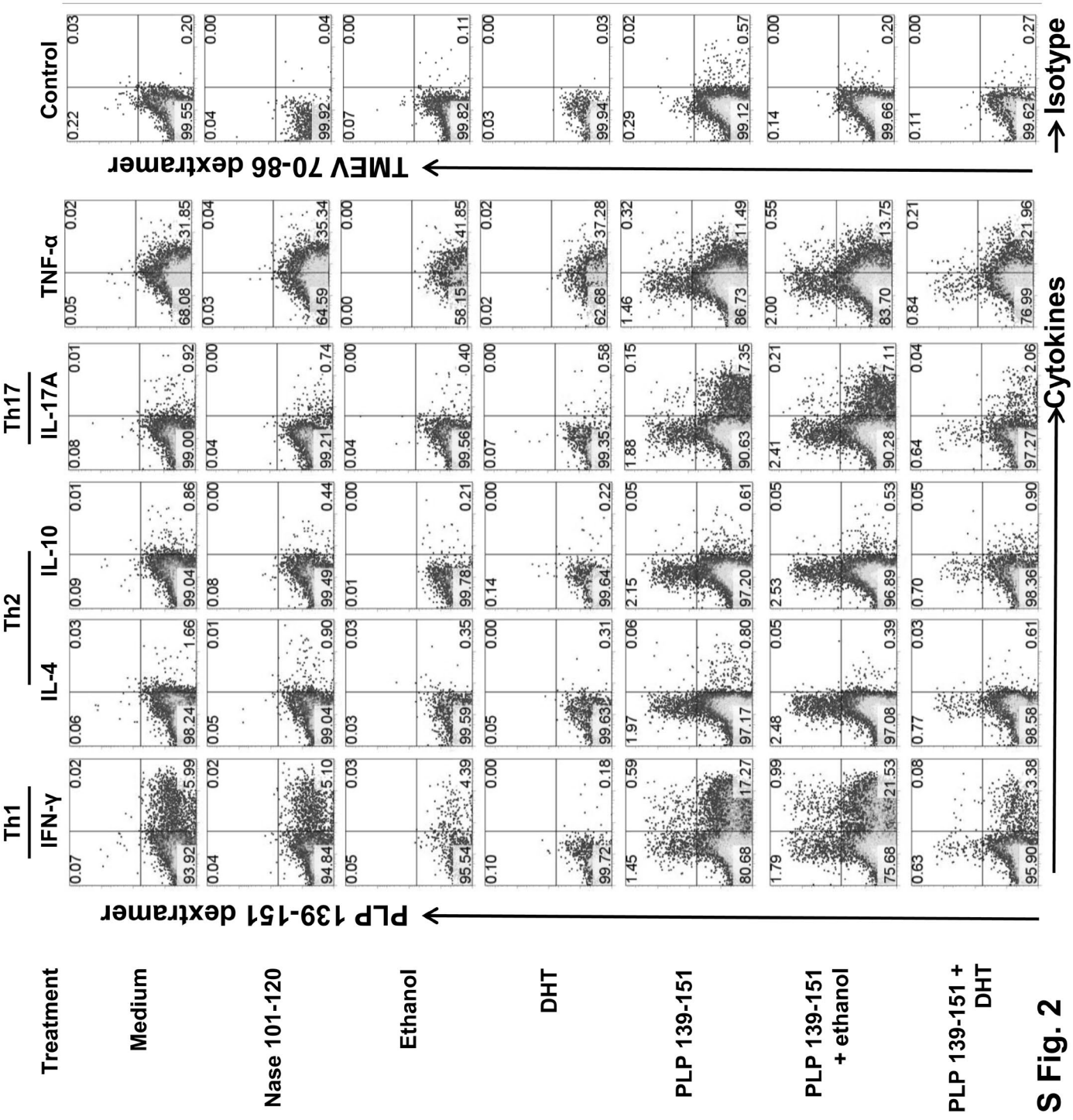
Treatment
Medium
Nase 101-120
Ethanol
DHT
PLP 139-151
PLP 139-151 + ethanol
PLP 139-151 + DHT
Th1
IFN-γ
Th2
IL-4
IL-10
Th17
IL-17A
TNF-α
PLP 139-151 dextramer
TMEV 70-86 dextramer
Control
Cytokines
Isotype

S Fig. 2

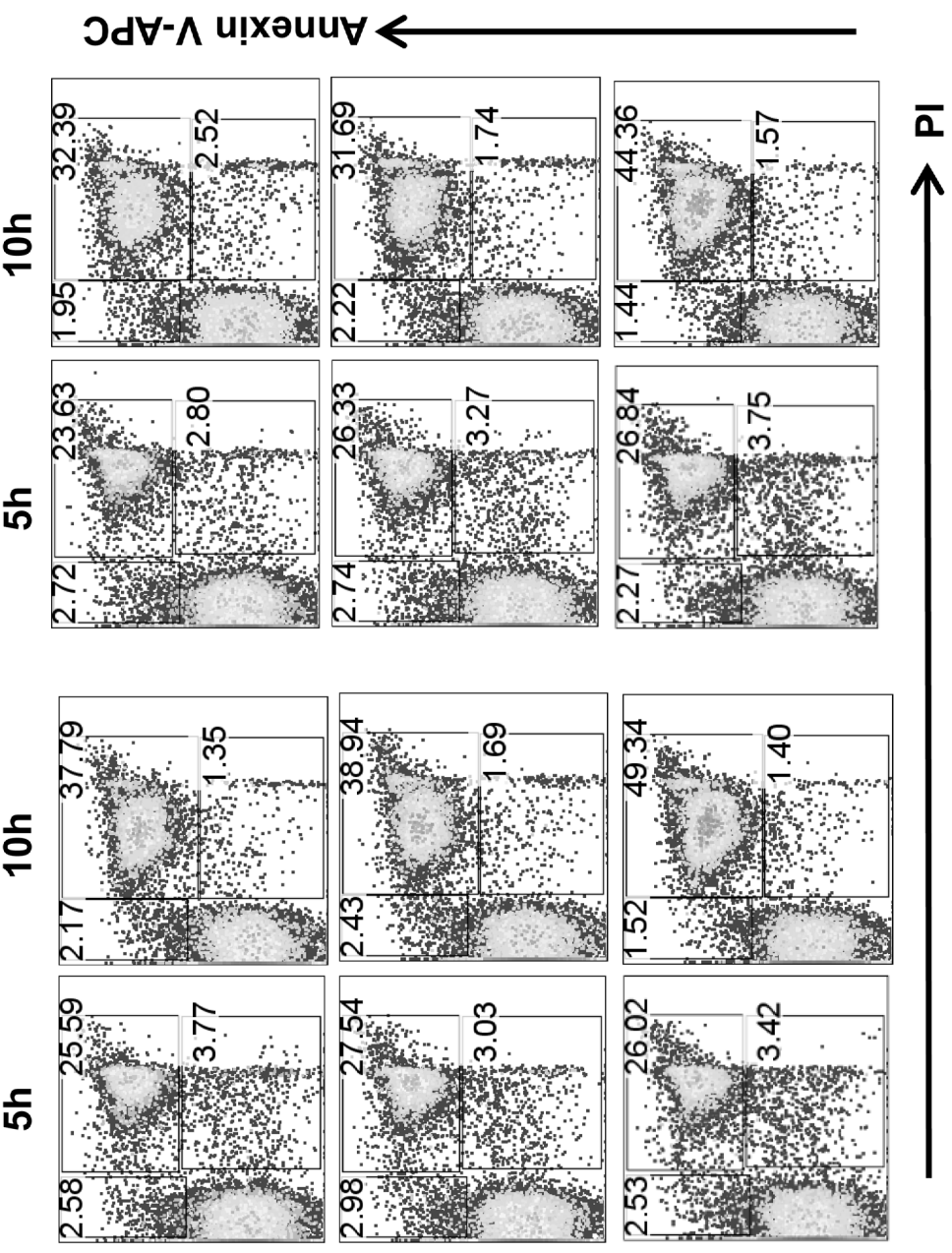
Unstimulated
Stimulated with anti-CD3
5h
10h
Treatment
Medium
Ethanol
DHT
Annexin V-APC
PI
2.58
25.59
3.77
2.17
37.79
1.35
2.98
27.54
3.03
2.43
38.94
1.69
2.53
26.02
3.42
1.52
49.34
1.40
2.72
23.63
2.80
1.95
32.39
2.52
2.74
26.33
3.27
2.22
31.69
1.74
2.27
26.84
3.75
1.44
44.36
1.57

S Fig. 3

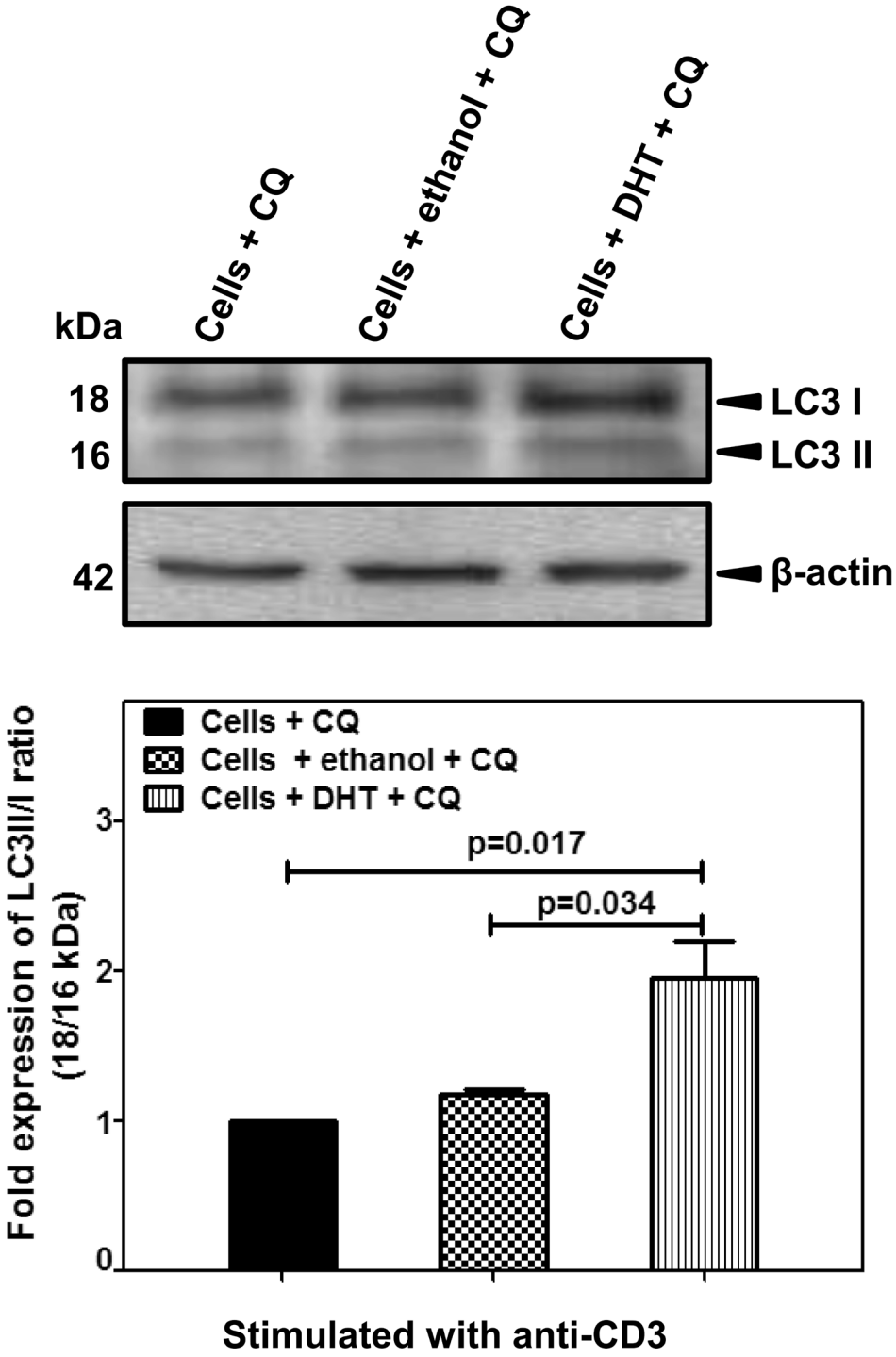
Cells + CQ
Cells + ethanol + CQ
Cells + DHT + CQ
kDa
18
16
LC3 I
LC3 II
42
β-actin
Cells + CQ
Cells + ethanol + CQ
Cells + DHT + CQ
p=0.017
p=0.034
Fold expression of LC3II/I ratio (18/16 kDa)
0
1
2
3
Stimulated with anti-CD3

S Fig. 4

Supplementary Table 1 Analysis of cell death in LNCs stimulated with or without PLP 139-151 and DHT

Group	PLP 139-151 (μg/ml) / DHT (nM)											
	2.5		5		10		20		40		80	
	Apoptotic cells	Dead cells	Apoptotic cells	Dead cells	Apoptotic cells	Dead cells	Apoptotic cells	Dead cells	Apoptotic cells	Dead cells	Apoptotic cells	Dead cells
Medium	1.4 ± 0.1	65.7 ± 1.8	1.4 ± 0.1	65.7 ± 1.8	1.4 ± 0.1	65.7 ± 1.8	1.4 ± 0.1	65.7 ± 1.8	1.4 ± 0.1	65.7 ± 1.8	1.4 ± 0.1	65.7 ± 1.8
Nase	1.5 ± 0	63.6 ± 2.4	1.6 ± 0.1	63.9 ± 1.5	1.6 ± 0.1	65.5 ± 2.4	1.7 ± 0.2	65 ± 2.8	1.7 ± 0.2	65.2 ± 1.5	1.9 ± 0.2	63.4 ± 1.6
Ethanol	1.5 ± 0.1	67 ± 2.1	1.5 ± 0.1	68.1 ± 2.5	1.4 ± 0.1	68.1 ± 2.9	1.4 ± 0.1	68.3 ± 1.5	1.4 ± 0.1	68.7 ± 1.8	1.5 ± 0	70.1 ± 0.5
DHT	1.4 ± 0.1	73.1 ± 2.5	1.5 ± 0.1	73.1 ± 1.9	1.3 ± 0.1	82.3 ± 0.7[a]	1.2 ± 0.2	84.5 ± 3[a]	1 ± 0.1	92.3 ± 0.5[a]	0.9 ± 0[a]	95.2 ± 0.2[a]
PLP	1.6 ± 0.1	61.4 ± 1.4	1.7 ± 0.1	59.6 ± 1.7	1.8 ± 0.3	59.3 ± 1.6	1.9 ± 0.1	58.2 ± 1.3	1.7 ± 0.1	59.7 ± 1.3	1.9 ± 0.2	57 ± 0.9
PLP + ethanol	1.6 ± 0	61.6 ± 0.9	1.5 ± 0.2	59.7 ± 1.1	1.8 ± 0.2	58.7 ± 2.1	1.7 ± 0.1	57.9 ± 0.5	1.8 ± 0.2	55.4 ± 1.3	1.8 ± 0.1	57.8 ± 1.9
PLP + DHT	1.1 ± 0[b]	65.6 ± 1.4	1.2 ± 0.1	63.1 ± 0.9	1.2 ± 0.1	65.9 ± 1.2[b]	1 ± 0.1[b]	71 ± 1.6[b]	0.7 ± 0.2[b]	76.5 ± 1.8[b]	0.5 ± 0.1[b]	84 ± 3.4[b]

[a]represents comparisons between DHT and ethanol groups ($p \leq 0.007$)

[b]represents comparisons between PLP + DHT, and PLP + ethanol groups ($p \leq 0.041$)

Supplementary Table 2 Analysis of cell death in LNCs stimulated with or without anti-CD3 and DHT and torin-1

Group	Unstimulated		Stimulated with anti-CD3	
	Apoptotic cells	Dead cells	Apoptotic cells	Dead cells
Cells	2.6±0.2	52.6±0.7	2.7±0.3	48.9±1.7
Cells + ethanol	2.5±0.3	54.3±0.6	2.2±0.3	48.5±1
Cells + DHT	2.2±0.3	67.1±0.9[a]	2.1±0.2	59.1±1.6[a]
Cells + DMSO	2.4±0.3	55.8±0.7	2.3±0.3	49.4±1.1
Cells + torin-1	2.2±0.2	59.9±0.7[b]	2.2±0.3	55.2±1.8[b]
Cells + ethanol + DMSO	2.2±0.1	56.9±1.2	2.1±0.2	49.9±1
Cells + DHT + torin-1	2±0.1	70.1±0.6[c]	2.1±0.1	64.7±1.2[c]

[a]represents comparisons between cells + DHT, and cells + ethanol groups ($p \leq 0.005$)
[b]represents comparisons between cells + torin-1, and cells + DMSO ($p \leq 0.028$)
[c]represents comparisons between cells + DHT + torin-1, and cells + ethanol + DMSO groups($p \leq 0.011$)